AD-A137 087 SOME PRELIMINARY THEORETICAL AND EXPERIMENTAL STUDIES ON UNDULATED OPEN TUBULAR FLOW PATHS(U) DAYTON UNIV OH RESEARCH INST W A RUBEY ET AL. SEP 82 UDR-TR-81-157 1/1

UNCLASSIFIED AFWAL-TR-82-2077 F/G 20/4 NL

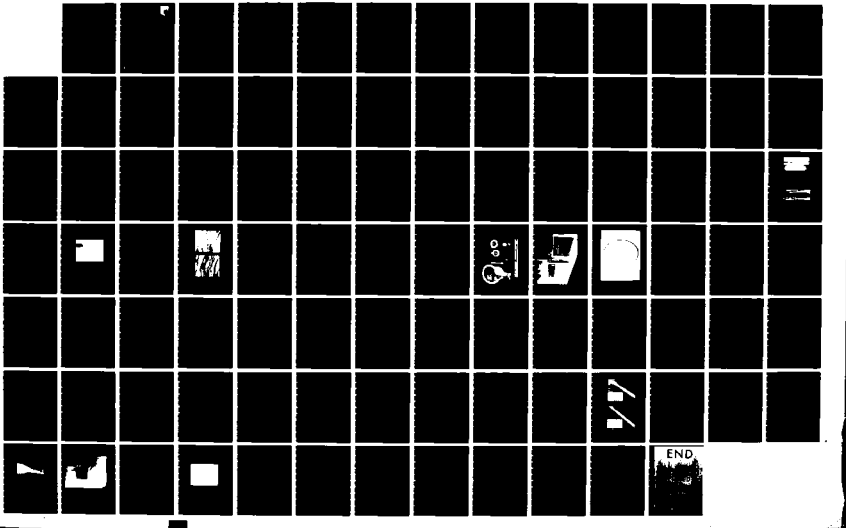

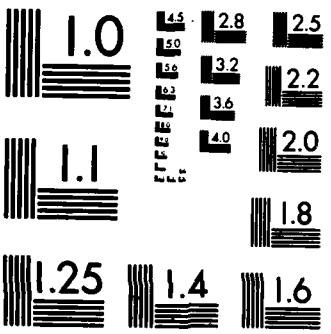

AFWAL-TR-82-2077

SOME PRELIMINARY THEORETICAL AND EXPERIMENTAL STUDIES ON UNDULATED OPEN TUBULAR FLOW PATHS

Wayne A. Rubey, L. Krishnamurthy, and
William E. Dirkes, Jr.

UNIVERSITY OF DAYTON RESEARCH INSTITUTE
300 COLLEGE PARK AVENUE
DAYTON, OHIO 45469

September 1982

FINAL REPORT FOR PERIOD APRIL 1981 - NOVEMBER 1981

Approved for Public Release; Distribution Unlimited

AERO PROPULSION LABORATORY
AIR FORCE WRIGHT AERONAUTICAL LABORATORIES
AIR FORCE SYSTEMS COMMAND
WRIGHT-PATTERSON AIR FORCE BASE, OHIO 45433

NOTICE

When Government drawings, specifications, or other data are used for any purpose other than in connection with a definitely related Government procurement operation, the United States Government thereby incurs no responsibility nor any obligation whatsoever; and the fact that the government may have formulated, furnished, or in any way supplied the said drawings, specifications, or other data, is not to be regarded by implication or otherwise as in any manner licensing the holder or any other person or corporation, or conveying the rights or permission to manufacture, use, or sell any patented invention that may in any way be related thereto.

The data in this report are a factual presentation of the results of the particular tests performed. They do not constitute official endorsement, condemnation, or approval of these products. The results in this report are not to be used, copied, or referenced for advertisement purposes.

This report has been reviewed by the Office of Public Affairs (ASD/PA) and is releasable to the National Technical Information Service (NTIS). At NTIS, it will be available to the general public, including foreign nations.

This technical report has been reviewed and is approved for publication.

DONALD D. POTTER, MAJOR, USAF
Fuels Branch, Fuels & Lubr Div
Aero Propulsion Laboratory

ARTHUR V. CHURCHILL
Chief, Fuels Branch
Fuels and Lubrication Division
Aero Propulsion Laboratory

FOR THE COMMANDER:

ROBERT D. SHERRILL
Chief, Fuels and Lubrication Division
Aero Propulsion Laboratory

"If your address has changed, if you wish to be removed from our mailing list, or if the addressee is no longer employed by your organization, please notify AFWAL/POSF, W-PAFB, OH 45433 to help us maintain a current mailing list."

Copies of this report should not be returned unless return is required by security considerations, contractual obligations, or notice on a specific document.

UNCLASSIFIED

SECURITY CLASSIFICATION OF THIS PAGE (When Data Entered)

REPORT DOCUMENTATION PAGE		READ INSTRUCTIONS BEFORE COMPLETING FORM
1. REPORT NUMBER AFWAL-TR-82-2077	2. GOVT ACCESSION NO. A137057	3. RECIPIENT'S CATALOG NUMBER
4. TITLE (and Subtitle) SOME PRELIMINARY THEORETICAL AND EXPERIMENTAL STUDIES ON UNDULATED OPEN TUBULAR FLOW PATHS		5. TYPE OF REPORT & PERIOD COVERED Final Report for Period April 1981 - November 1981 6. PERFORMING ORG. REPORT NUMBER UDR-TR-81-157
7. AUTHOR(s) Wayne A. Rubey, L. Krishnamurthy, and William E. Dirkes, Jr.		8. CONTRACT OR GRANT NUMBER(s) F33615-81-K-2043
9. PERFORMING ORGANIZATION NAME AND ADDRESS University of Dayton Research Institute 300 College Park Avenue Dayton, OH 45469		10. PROGRAM ELEMENT, PROJECT, TASK AREA & WORK UNIT NUMBERS P.E. 61102F Project 2303 SI 07
11. CONTROLLING OFFICE NAME AND ADDRESS Aero Propulsion Laboratory (AFWAL/POSF) Air Force Wright Aeronautical Laboratories (AFSC) Wright-Patterson Air Force Base, Ohio 45433		12. REPORT DATE September 1982 13. NUMBER OF PAGES 83
14. MONITORING AGENCY NAME & ADDRESS(if different from Controlling Office)		15. SECURITY CLASS. (of this report) Unclassified 15a. DECLASSIFICATION/DOWNGRADING SCHEDULE

16. DISTRIBUTION STATEMENT (of this Report)

Approved for public release; distribution unlimited

17. DISTRIBUTION STATEMENT (of the abstract entered in Block 20, if different from Report)

18. SUPPLEMENTARY NOTES

19. KEY WORDS (Continue on reverse side if necessary and identify by block number)

gas chromatography
open tubular columns
flow visualization
fluid dynamics
glass drawing
nozzle
diffuser

20. ABSTRACT (Continue on reverse side if necessary and identify by block number)

Theoretical and experimental investigations were conducted to evaluate the fluid dynamic behavior of flows in undulated open tubes (UOT). The UOT concept was evaluated to determine whether or not it could be used to improve the performance of gas chromatography. Gas chromatography is an analytical technique which can be used to separate, identify, and quantitate the components of complex mixtures such as jet fuels. Gas chromatographic data is usually displayed as signal strength plotted versus retention time. The individual compounds in the mixture are separated into solute zones in the gas chromatographic column; these

DD FORM 1 JAN 73 1473

UNCLASSIFIED

SECURITY CLASSIFICATION OF THIS PAGE (When Data Entered)

ABSTRACT cont'd.

solute zones are represented as peaks on the data plot. Gas chromatographic performance is improved by decreasing the width of the individual peaks, increasing the separation between neighboring peaks, and increasing the amount of sample which can be injected without causing peak distortion. In general, these three goals cannot be achieved simultaneously; gas chromatograph design requires compromise among these three goals. The focus of this effort was to determine whether an undulated open tube could allow narrower peaks (reduced solute zone dispersion) and larger sample capacities than state-of-the-art capillary columns. An undulated open tube is circular in cross-section, but the diameter decreases then increases in a repetitive manner along the length of the tube, producing a repetitive nozzle/diffuser flowpath.

Flow visualization techniques were used to evaluate the fluid dynamic behavior of the UOT at Reynolds numbers less than 200 with liquid flows. Metal UOT samples were fabricated and their zone dispersion behavior was evaluated using gaseous flow. Techniques for fabricating UOT samples from glass were investigated. Experiments showed that the UOT samples evaluated did not display improved chromatographic performance when compared with state-of-the-art chromatographic columns.

A UOT

PREFACE

The report was prepared by the Environmental Sciences Group and the Fluid Mechanics Group of the University of Dayton Research Institute, University of Dayton, Dayton, Ohio. The work reported herein was conducted under Contract No. F33615-81-K-2043 which was funded by the Air Force Wright Aeronautical Laboratories, Aero Propulsion Laboratory.

The Co-Principal Investigators for this research activity were Mr. Wayne A. Rubey and Dr. L. Krishnamurthy and the Technical Monitor was Major Donald D. Potter, Aero Propulsion Laboratory.

This research program was initiated in April 1981 and was completed in October 1981.

TABLE OF CONTENTS

LIST OF ILLUSTRATIONS

LIST OF TABLES

LIST OF SYMBOLS

a	constant (= arctanh $(2/3)^{1/2}$) in the Pohlhausen velocity distribution for purely radial flow
b	constant which is a measure of the amplitude of the local constriction of the symmetric bell-shaped type
c	constant which is a measure of the sharpness of the local constriction in the above
D	diameter of the uniform circular tube
D_e	diameter of the entrance region
D_E	equivalent diameter for a divergent channel = $4r \sin \alpha$
F	velocity distribution function due to Pohlhausen for the purely radial flow
L	length of entrance region
L_{99}	length of tube where the local axial velocity is 99% of the fully-developed value
P_w	wall static pressure
Q	volume flow rate
r	radial distance from the axis
R	radius of the uniform circular tube
R_e	Reynolds number = UD/ν
u	axial velocity at any radial location
U	mean axial velocity; also the axial velocity at the axis
U_m	maximum axial velocity at the axis
x	axial distance along the flowpath
X	nondimensional parameter (= $U_m r/\nu$)
z	axial distance
α	half angle of divergence
θ	angular coordinate
ν	kinematic viscosity of the fluid
ρ	density of the fluid

Subscripts

L denotes laminar flow condition

T denotes turbulent flow condition

w denotes wall condition

2 denotes conditions at the small diameter section downstream of the contraction

Superscripts

n exponent for the power-lane velocity profile for fully-developed pipe flow

* denotes critical flow condition beyond which flow separation occurs

SECTION I

INTRODUCTION

Gas chromatography (GC) is a powerful analytical technique for analyzing complex mixtures of volatile organic compounds. GC is used to separate, identify, and quantitate the components of complex mixtures such as jet fuels. The individual components in a typical mixture are separated into solute zones by the gas chromatographic column, and the solute zones are eventually displayed as individual concentration profiles, or peaks, on the output data plot. The most important single component in a gas chromatograph is the separation column[1,2]. Packed columns have a high sample capacity, but they generally produce low resolution separations. Capillary columns exhibit low sample capacity, but are capable of producing high-resolution separations. A typical high-resolution gas chromatography (HRGC) separation column is of open tubular construction and has a uniform narrow bore. The inner surface of this tubing is normally coated with a thin film of non-volatile liquid, usually polymeric in nature. It is unfortunate that the resolving power of the present columns is inversely proportional to bore diameter[3,4]. Hence, the small diameter columns that provide good resolution have both a low sample capacity and a high pressure drop.

Based upon a reexamination of a basic gas chromatographic column from a fluid mechanics viewpoint, a new and different type of chromatographic column has been contemplated. From what is presently known from chromatographic theory and fluid mechanic considerations, this conceptualized high-resolution column, known as an undulated open tubular column (UOTC), could overcome certain limitations associated with the small bore open tubular columns of today. If this new type of GC column proves successful, then GC analyses could be conducted:

(a) with greater resolution,

(b) in a shorter elapsed time,
(c) with greatly enhanced sensitivity for trace components, and
(d) with less operational difficulties.

In short, if the UOTC concept was successful, a greater analytical capability would be forthcoming in HRGC.

Many researchers have theorized as to what might be the best cross-sectional profile for an HRGC column[4-7]. We have also given considerable thought to this intriguing topic (see Figure 1), and for some time now we have been of the opinion that the circular cross-section is the optimum geometrical configuration. Other theoretical investigations[8] are also coming to the same conclusion. Even so, almost no consideration has been given as to what would be the optimum geometrical configuration in the axial direction of an optimized HRGC column. The straight uniform cylindrical bore is the easiest to fabricate and treat theoretically. Also, the general opinion is that this configuration is best. However, based upon some of our studies and reviews of the early literature dealing with fluid flow through nozzles and diffusers, we were not convinced that the uniform cylindrical bore would, indeed, produce the optimum performance. In fact, we felt that an unduloidal surface might have some very beneficial properties with respect to enhanced transport and chromatographic behavior.

At this point it is necessary to define some terms that will be frequently used throughout the remainder of this technical report. Undulating basically means having a wavelike form or motion. Unduloids are geometrical forms; specifically, the only radially symmetrical surfaces of constant mean curvature which may be extended axially without limit are known as the unduloids. The cylinder and sphere are limiting cases of unduloids[9]. An unduloidal surface is merely the three dimensional surface represented by unduloids. We will be referring to modified unduloidal surfaces throughout this technical report, and we consider the nozzle/diffuser type of configuration as a modified unduloidal surface. We will refer to such tubing as an undulated open tube

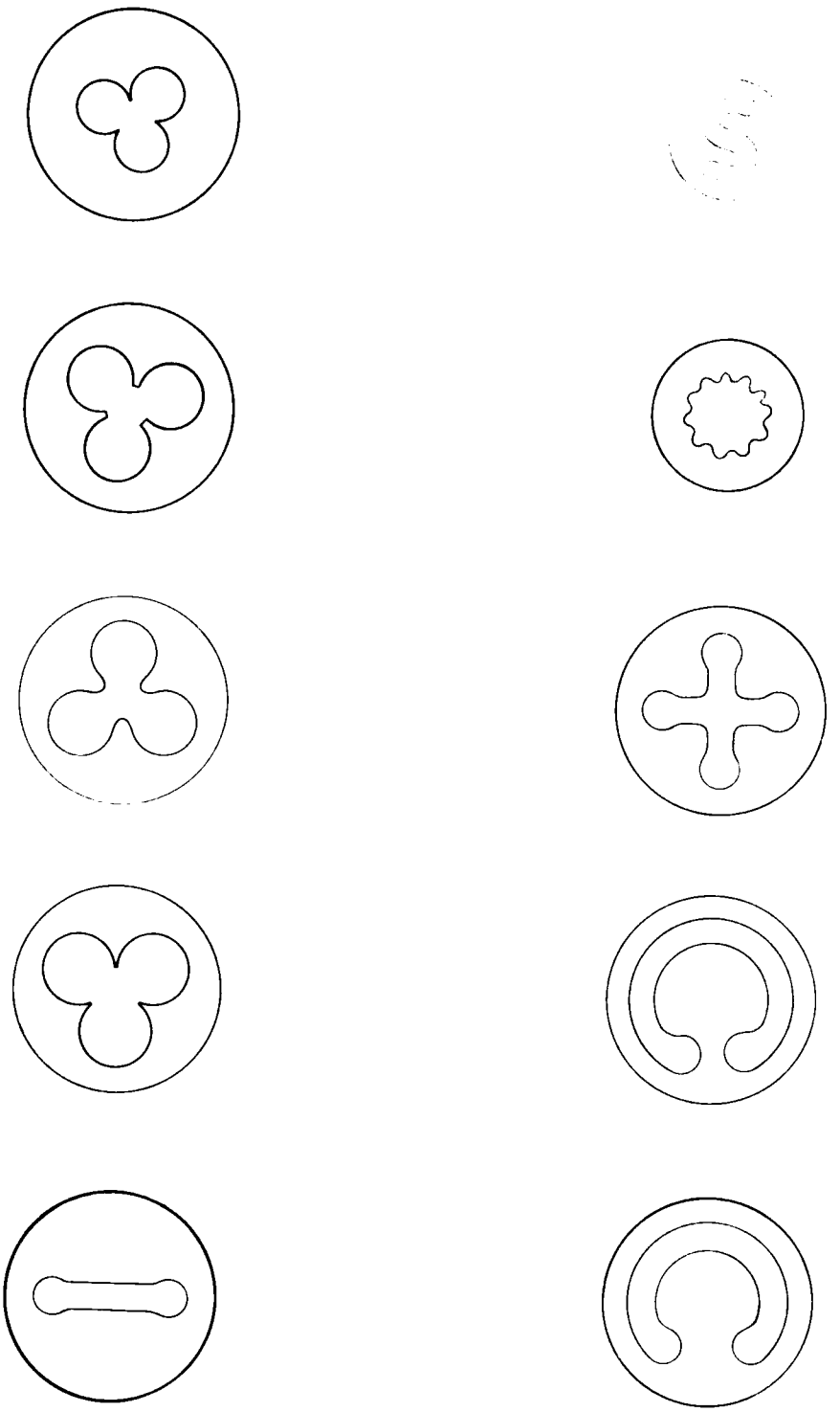

Figure 1. Variety of tubular cross-sections.

(UOT) and a column made from this tubing will be referred to as an undulated open tubular column (UOTC).

The flow of a fluid through an undulated tubular flowpath is somewhat unique and unnatural. It is unnatural in the sense that practically every type of naturally occurring gas or liquid transport passageway, e.g., in plants, vegetation, physiological species, etc., is essentially of relatively uniform open cylindrical configuration. However, there are many instances when the openness and cross-sectional area of these tubular passageways varies with time, e.g., that encountered in pulsating fluid flow in flexible passageways such as blood vessels.

Fundamentally, an undulated fluid flowpath has not been studied in detail. Thus, a narrow and long unduloidal flowpath consisting of repetitive nozzle/diffuser configurations presents some intriguing properties with respect to transporting fluids.

SECTION II

BACKGROUND AND RELATED RESEARCH STUDIES

The basic concept that is the subject of this technical report draws heavily upon research studies that have been conducted in two different technical fields; namely, open tubular column gas chromatography and fluid mechanics. The discussion that follows will point out some of the more significant and relevant work in these two areas, specifically as they apply to an undulated open tubular column.

1. Open Tubular Gas Chromatographic Studies

There have been several extensive studies conducted which describe the dynamic behavior of solute zones as they migrate through a chromatographic separation column[10-14]. Some of these studies date to the middle 1950's. Also, some of the classic works which describe dispersive behavior in fluid transport date to that same period[15,16]. The relevant papers of Golay[12-14] were presented around 1957. He also theorized, at that time, as to what might be the ideal gas chromatographic column[13]. He indicated that a coated open tubular column with a velvet-like interior surface would produce optimized gas chromatographic behavior.

Over the years, the performance aspects of a wide variety of chromatographic column designs have been studied and characterized[16-20]. In addition to the above studies, which basically characterized the behavior of various separation columns, there have been several fundamental investigations conducted which focused attention primarily upon the ultimate performance of both gas and liquid chromatographic columns[21-24]. These investigations were theoretical in nature, and were based upon fundamental physiochemical and fluid transport relationships. The results of these investigations have clearly indicated that there are upper bounds with respect to chromatographic performance.

However, at the present time we are operating at performance levels significantly lower than the predicted upper limitations.

Preparative gas chromatography has been forced to use wide bore packed columns[25,26] in an effort to obtain large throughputs. Consequently, chromatographic efficiency has been sacrificed as the relatively large diameters of these separation columns, and the sizeable variation in the gas velocities through the packed media have greatly contributed to the longitudinal dispersion of migrating solute zones. Even so, these preparative GC studies have been enlightening as they have determined the mechanisms by which dispersion in these large diameter columns takes place. Also, up to now, almost all preparative columns have indeed been of the packed column variety. Several packed column studies have been conducted which characterized lateral diffusion and local nonequilibrium behavior[27-29]. These same characterizations have been applied in the miniaturized realm of open tubular column chromatography. In addition, advances[23] continue to be made in the study of dispersion mechanisms and band spreading phenomena.

The chromatographer has always wanted to obtain his analytical data faster and with greater resolution. Thus, one approach that researchers have pursued is turbulent flow gas chromatography. Two excellent studies[30,31] conducted in this area concur that although this is an interesting field of inquiry, it has some definite practical limitations; very high pressures are needed to maintain turbulent flow in a gas chromatographic column.

Another approach to obtaining high-resolution separations, both in gas chromatography and liquid chromatography, has been to induce (or exploit) secondary flow behavior in the fluid flow path. Many researchers have examined this interesting behavior with respect to chromatography[32-36]. They have studied this phenomenon both from a theoretical standpoint and with actual experiments using tightly coiled helical tubes. Again, this is a very intriguing area, but it is one that is faced with tremendous

practical consequences and physical barriers. It is very difficult to coil tubing into very tight helices. These tight helices are necessary for inducing the centrifugal forces required to produce adequate secondary flow in the flow path. Both of these previously mentioned approaches tend to flatten the usual parabolic velocity distribution of the flowing fluid. Turbulent flow definitely produces a flatter velocity profile and, of course, secondary flow would alter the parabolic velocity distribution to a considerable extent.

Before moving on to the next topic of chromatographic research, it would be well to remember that, what has been stated thus far has been with respect to circular cross-section fluid flow paths. In Golay's second paper on capillary column gas chromatography[14], the behavior of a rectangular cross-section capillary column was described. In this paper, the ends of the tubing cross-section were considered to have negligible effect upon chromatographic performance. This is an important point because, although it may have a somewhat negligible effect from chromatographic standpoints, it is far from negligible with respect to fluid mechanic considerations and also transport processes.

Only recently have chromatographers followed up on Golay's suggestion of actually preparing and using a rectangular cross-section open bore column. Several experimenters have constructed such tubing and examined the zone dispersive behavior of these tubes[5-8,37]. In reality, rectangular cross-section tubing does present a relatively efficient flow path with respect to minimizing dispersion. However, it does so at the expense of a considerable increase in pressure drop.

Other cross-sections[38] have also been examined, e.g., ovalized and various elliptical cross-sections. In liquid chromatography, a variety of tubing cross-sections and crimped tubes have been studied[39-41]. Some benefits have been observed, but these observations were made with tubes that would not rival a typical high efficiency separation column. Throughout these

studies the effects of longitudinal variations have been examined to some extent but, in every case they have utilized some form of crimping action thereby introducing a cross-section other than circular. Several investigators have tried to introduce a certain degree of mixing or intentionally breaking up the parabolic velocity distribution; but in so doing, they have probably introduced uncontrolled eddy currents and produced unswept regions which would result in poor chromatographic performance.

Conical shaped packed columns[42,43] have been studied briefly; however, these are relatively long conical lengths and they do not in any way take advantage of possible beneficial fluid mechanical properties. It must be remembered that these conical shaped packed columns would exhibit frontal flow behavior. Other types of innovations are still being applied in the design of chromatographic columns to improve performance, either with respect to speed of analysis or with respect to obtaining greater separation capabilities.

Two areas that have been recently introduced, and are still receiving attention with respect to possible future applications, are the flow segmentation principle[44] as applied to coated open tubular columns, and the application of super critical fluids[45]. In the latter application, gases are used at extremely high pressure which permits the gaseous mobile phase to behave in a manner very similar to liquids.

A variety of attempts have been made to utilize the beneficial aspects of hydrodynamic phenomena to obtain improved chromatographic performance. These procedures[46-48] have been applied primarily in a special type of liquid chromatography separation. These procedures have also found application in the separation of various colloidal materials. In fact, a special type of separation technique known as hydrodynamic chromatography has evolved from this work. One should remember that this particular technique is really not a chromatographic technique in the proper sense of the word, as there is only one phase

involved in this separation procedure. Basically, chromatographic separations are made by interaction of the migrating solutes between two phases, i.e., a stationary phase and a mobile phase.

Hydrodynamic phenomena have also been observed, to some extent, in gas chromatography, particularly in the technique known as packed capillary column gas chromatography[17]. In this technique, sizeable fixed particles attached to the walls of the relatively open flow path tend to disrupt the parabolic velocity distribution, and a certain degree of mixing is encountered. In some aspects this has been found to be beneficial. It has not yet found wide utilization in gas chromatography, although this type of an approach may eventually be utilized in very fine bore liquid chromatography.

2. Fluid Dynamic Studies

It was noted earlier that the undulated open tubular column under consideration herein represents an internal flow path of circular cross section that is alternately converging and diverging in the longitudinal direction. Thus, unlike the conventional open tubular column which is a uniform circular tube, the UOTC comprises a large number of nozzle/diffuser elements forming the flow path. The fluid dynamic behavior of the internal flow in a circular tube is well known in both laminar and turbulent flow regimes (see Ward-Smith[49], for example). This is especially true of the flowfield corresponding to the so-called fully-developed flow which gives rise to the Hagen-Poiseuille velocity profile in the laminar flow and the power-law profile in the turbulent flow. Indeed, the parabolic velocity profile in the fully developed laminar flow has been the starting point of a number of theoretical analyses relating to the dispersive behavior of flow in tubes[15,16,50] and also forms the basis of the open tubular column chromatography[3]. On the other hand, it appears from a review of the literature that there has been no examination of the fluid dynamic characteristics of the UOT.

Thus, no theoretical and experimental information is available on UOT flowfields which can facilitate the chromatographic examination of this flow path. However, some information is available on the fluid dynamic characteristics of the component parts of the UOT--the nozzle and the diffuser. A brief review of this information is outlined here to the extent it is relevant to the fluid dynamic investigation of the UOT.

It must be noted here that a single nozzle/diffuser element resembles the venturi tube, which is a well-known flow-metering device. Unfortunately, the design information that has been established for the venturi tube relates more to its role as a flowmetering device than as a UOT component. The main reason for this situation is that the practical interest in flowmetering is largely confined to turbulent flows. The same is also true of much of the available information on convergent and divergent flow paths. Thus, any inclusion here of turbulent flow regimes is not expected to have direct relevance to our understanding of the UOT configuration. Our emphasis here is on laminar flows since the Reynolds numbers under typical conditions of open tubular column gas chromatography are less than 1×10^3 and the same is expected to be true of an UOTC as well.

The steady laminar flow of an effectively incompressible fluid in a straight tube of constant cross-section attains a velocity profile which becomes eventually independent of the axial distance. The flow is said to have become fully developed for which the Navier-Stokes equations readily yield the exact solution giving rise to the well-known parabolic velocity distribution. Experiments have established the validity of this result for flow Reynolds numbers less than about 2,000 when the flow is laminar. This Hagen-Poiseuille velocity distribution may be expressed as

$$(u/U)_L = 1 - r^2/R^2,$$

where U is the velocity (maximum) at the axis of the tube of radius R, and u is the velocity at any radial distance r from the axis. The subscript L denotes laminar flow. As noted earlier, this is the starting point for the Golay equation for the open tubular column.

The velocity distribution becomes more uniform at high Reynolds numbers where fully-developed turbulent flow is encountered. This corresponds to Reynolds numbers higher than 4,000. A power-law relation has been found to provide a good representation of the velocity profile. This may be expressed as

$$(u/U)_T = (1 - r/R)^{1/n},$$

where the exponent n is a function of the Reynolds number. Here the subscript T denotes the turbulent flow condition. The value of n has been found to be 6, 7, and 10, respectively for Reynolds numbers of 4×10^3, 100×10^3, and $3{,}240 \times 10^3$. In contrast with the laminar parabolic velocity profile, the tendency toward uniform velocity profiles in turbulent flows is evident from Table 1 which gives the Hagen-Poiseuille and power-law velocity profiles. The power-law profiles are given for four different values of n.

It is well known that the increasing tendency to more uniform velocity distribution in turbulent flows arises from the enhanced momentum transfer from the faster moving fluid in the middle of the tube to the slower moving fluid near the wall. This increase is due to momentum transport by turbulent eddies which is much larger than the molecular transport occurring in laminar flows. However, the chromatographic need to retain laminar flow implies that the improvement over the parabolic velocity distribution must be achieved by means other than the introduction of turbulence.

It was stated earlier that the fully-developed velocity profile occurs after a certain distance from the beginning of the tube. For example, flow through the open tubular column may

TABLE 1

FULLY DEVELOPED LAMINAR AND TURBULENT
VELOCITY PROFILES IN CIRCULAR TUBES

		$(u/U)_T = (1 - r/R)^{1/n}$			
r/R	$(\frac{u}{U})_L = 1 - \frac{r^2}{R^2}$	n = 5	6	7	10
0	1	1	1	1	1
0.1	0.99	0.979	0.983	0.985	0.99
0.2	0.96	0.956	0.963	0.969	0.978
0.3	0.91	0.931	0.942	0.950	0.965
0.4	0.84	0.903	0.918	0.930	0.950
0.5	0.75	0.871	0.891	0.906	0.933
0.6	0.64	0.833	0.858	0.877	0.912
0.7	0.51	0.786	0.818	0.842	0.887
0.8	0.36	0.725	0.765	0.795	0.851
0.9	0.19	0.631	0.681	0.720	0.794
1.0	0	0	0	0	0

begin from a reservoir of much larger dimensions. The velocity profile at the entry depends on the conditions at, and immediately upstream of, the entrance region. But the entry profile which can be made virtually uniform (by a suitable design of the reduction in cross section from the reservoir to the tube) has significant influence only for the first two or three diameters of the tube. The subsequent flow development remains largely unaffected by the entrance conditions, and the flow asymptotically attains the fully-developed condition solely due to viscous effects. The distance through which the fluid must move before becoming fully established is called the entrance length and for practical purposes it is defined to be the distance at which the velocity on the axis attains 99 percent of the fully-developed value. This length, denoted by L_{99}, has been found to depend on the Reynolds number. For Reynolds numbers below 500, Friedman et al.[51] have determined the entrance lengths by the numerical solution of the complete Navier-Stokes equations. These results are shown in Table II. Here the Reynolds number is given by $Re \equiv UD/\nu$ where ν is the kinematic viscosity of the fluid, $D = 2R$ is the diameter of the tube, and $U = Q/\pi R^2$ is the mean flow velocity, Q being the volume flow rate. Friedman et al. have obtained the results for $Re = 0$ from an analytical solution of the Navier-Stokes equations and for $Re = \infty$ by extrapolation.

We can easily estimate the entrance length for typical open tubular columns. Consider a column diameter of 1 mm and gases such as hydrogen or helium (whose kinematic viscosities at 27°C are respectively 1.034 and 1.22 cm^2/s). Thus, for a mean flow velocity of 1.0 m/s, the Reynolds number is about 10. This implies that the entrance length required to establish the parabolic profile is of the order of just one tube diameter. This conclusion has far reaching implications on our approach to eliminate the parabolic velocity profile, while retaining the laminar flow of the fluid. It is clear then that the axial profile variation in the tube must occur in distances of the order of one diameter in order to approach uniform velocity distribution.

TABLE 2

ENTRANCE LENGTH FOR LOW REYNOLDS NUMBERS

Re	L_{99}/D	$L_{99}/(D\ Re)$
0	0.6	---
10	0.88	0.088
20	1.35	0.0675
40	2.44	0.061
100	5.56	0.0565
150	8.48	0.0565
200	11.3	0.0565
300	16.8	0.056
400	22.4	0.056
500	28	0.056
∞	---	0.056

The one laminar-flow path component that tends to reduce the local nonuniformities in the axial velocity profile at a cross section (without the introduction of flow straighteners such as honeycombs, etc.) is a contraction or convergent nozzle. The characteristic geometrical feature of a contraction is the reduction of cross-sectional area with distance along the flow direction. While infinite contractions (wherein the walls become parallel to the axis asymptotically) or purely converging walls (wherein the flow is strictly radial) are usually studied in theory, the practical geometry of interest is the finite contraction. This consists of an upstream region where the tube wall is parallel to the flow axis, a region in which the cross section decreases, and a downstream region where the tube wall is again parallel to the flow axis.

Because of the area reduction in a contraction, it follows from the principle of conservation of mass that in incompressible flow there is a corresponding increase in the mean velocity as the fluid moves through the contraction. Furthermore, as can be seen by the application of the mechanical energy equation, there is a consequent decrease in the pressure. Thus, the laminar flow through the contraction may be broadly denoted as the flow through a favorable pressure gradient. It should be noted, however, that local regions of adverse pressure gradients (and even recirculating eddies) can occur in finite contractions even though the flow as a whole experiences favorable pressure gradients. Thus, judgement has to be exercised in choosing wall profiles of the contraction which can minimize the occurrence of adverse pressure gradients.

The increase in the mean axial velocity through the contraction results in the minimization of nonuniformities in the velocity profile. This can be seen easily from a control volume analysis of the flow through a contraction. Such an analysis shows that an upstream perturbation in the velocity profile is decreased downstream by a factor equal to the square of the area ratio of the contraction. The farther the departure

of the upstream velocity profile is from the Hagen-Poiseuille profile, the better is the uniformization downstream. Likewise, the so-called "throat" region downstream of the contraction must be short enough to avoid the flow again becoming fully developed.

A typical open tubular column has a diameter of the order of 1 mm and a length of the order of several meters. Thus, it is obvious that after the first contraction, the column must restore itself to the original diameter. This is accomplished by an increase in the cross section by means of an expansion which is a diverging section or a diffuser.

The geometrical feature characteristic of a diffuser is that its cross-sectional area increases along the flow direction. An immediate consequence of the principle of conservation of mass is that the mean velocity for an incompressible flow decreases through the diffuser. By a control volume analysis as in the case of contraction it can be seen that there is a tendency for the upstream nonuniformities to be maintained or even progressively magnified during the passage of the fluid through the diffuser. Thus, if the velocity profile at the entrance to the diffuser is parabolic, it is not likely to become more uniform downstream of the diffuser. This observation stresses the desirability of making the velocity profile upstream of the diffuser as uniform as possible.

A more serious consequence of the diffuser behavior in decreasing the flow velocity is the concomitant pressure increase from the entrance to the exit. Thus, the laminar flow through the diffuser takes place under an adverse pressure gradient. If the axial pressure gradient is large enough, the slower moving fluid in the boundary layer near the diffuser wall can separate and cause flow reversal near the wall. Both the flow Reynolds number and the angle of divergence of the diffuser determine the onset of flow separation. In view of this markedly distinct behavior of the flow in a diffuser in comparison with that in a nozzle, the choice of the diffuser wall profile and the angle of divergence requires even greater care.

A review of the literature has revealed that laminar flow in nozzles, diffusers, and combinations thereof has not received as much attention as turbulent flows. In particular, no definitive work appears to exist on the laminar diffusing flow in an axisymmetric geometry. This is somewhat surprising since its two-dimensional counterpart--the laminar flow between non-parallel (i.e., both converging and diverging cases) plane walls--has been studied long ago. Indeed, the so-called Jeffrey-Hamel flow which deals with purely radial flow (when the walls of the passage are sufficiently long, the flow becomes radial everywhere, except in the immediate vicinity of the entrance and the exit) is one of the very few topics for which the Navier-Stokes equations provide an exact solution. The solutions first obtained and analyzed by Jeffrey[52] in 1915 and by Hamel[53] in 1916 have been studied subsequently by a number of workers, the two main contributions being those of Rosenhead[54] and Millsaps and Pohlhausen[55]. The results of the analysis of the latter are quoted here. Consider the purely radial flow in a two-dimensional diverging channel of total angle of divergence 2α. A nondimensional parameter X can be defined as $X \equiv U_m r/\nu$, where U_m is the (maximum) velocity along the axis, r is the radial distance (from the origin where the diverging walls intersect), and ν is the kinematic viscosity. The critical value of X, denoted by X*, above which reverse flow can occur in the diffuser, is given by $X^* = (3.211/\alpha^*)^2$. This result may also be interpreted as providing, for a given X, the upperbound on the diffuser angle. Millsap and Pohlhausen have computed the velocity distribution in a diffuser with $\alpha = 5°$ for three values of X, viz., X = 5,000, X = X* = 1,342, and X = 684. For the highest value of X, backflow occurs over all angular coordinates (measured from the axis) greater than about 1.9°. In terms of a more conventional Reynolds number defined as $Re \equiv UD_E/\nu$, where U is the mean flow velocity in the axial direction, and D_E is the equivalent diameter given by $D_E = 4r \sin \alpha$, the critical Reynolds number Re* becomes $Re^* = 5.87 \sqrt{X^*}$. This result may also be expressed as $Re^* = 18.84/\sqrt{\alpha^*}$.

Thus, for a diffuser with $\alpha = 5°$, the critical Reynolds number above which separation and reverse flow will occur is about 216. Alternately, we can also determine the maximum angle of divergence for no separation to occur for a given Reynolds number. Thus, if the maximum Reynolds number encountered in the diffuser is known, then the largest permissible half angle of the diffuser is given by $\alpha^* = 18.84/Re^*$. Table 3 provides the results for some typical Reynolds numbers.

From the results shown in Table 3 it would appear that the Reynolds numbers in the range of 10 to 100 that are typical in open tubular column gas chromatography may tolerate fairly large angle of divergence in strictly radial, two-dimensional, laminar flow. We note that the foregoing results are valid for radial velocity distribution at the diffuser entry. Abramowitz[56] has investigated the situation where the entry velocity profile is parabolic, corresponding to the Hagen-Poiseuille velocity distribution (for two-dimensional flow) upstream of the diffuser. According to his analysis, the critical Reynolds number above which flow reversal first starts is given by $Re^*\alpha^* = 24.7$. This indicates that for a given diffuser, fully-established entry flow can tolerate Reynolds numbers that are about 31% higher than when the entry flow is radial. No analysis appears to exist for the case where the velocity profile is nearly uniform at the diffuser entrance as would occur if the diffuser is preceded by a convergent nozzle. Of course, the analysis and results quoted here are not valid for the axisymmetric geometry.

The two-dimensional, laminar flow between converging walls has also been analyzed for purely radial flow and an exact solution of the Navier-Stokes equations has been obtained for the velocity distribution. The original result due to Pohlhausen[57] for the velocity distribution $F(\theta)$ where θ is the angular coordinate may be expressed as follows:

$$F = X\{3 \tan h^2 [(X/2)^{1/2} (\alpha - \theta) + a] - 2\}$$

TABLE 3

OPTIMUM DIFFUSER HALF ANGLE FOR PURELY DIVERGING TWO-DIMENSIONAL FLOW

Re	α (in degrees)
20	54
50	21.6
100	10.8
200	5.4
500	2.16
1000	1.08

where α and X are as defined in the case of the diverging flow and $a = \text{arctanh}\ (2/3)^{1/2} = 1.146$. The above equation shows that F is approximately constant and equal to X, except within the wall-boundary layer, whose thickness is proportional to $(-X)^{-1/2}$. Note that the coordinate system and conventions adopted here (radially outward flow for diffuser and radially inward flow for the nozzle), X assumes negative values only for flow in a converging passage. In terms of the Reynolds number $Re = |U|\ D_E/\nu$ (the modulus of the mean velocity is introduced to keep Re positive), $Re \sim -4X\alpha$, ignoring the small correction for the boundary layer. When this relation is introduced in the expression for the velocity profile, an explicit relationship between the velocity profile and Reynolds number can be obtained. Such a relationship clearly shows that at sufficiently high Reynolds numbers the viscous effects are confined to a thin wall layer whose thickness is proportional to $Re^{-1/2}$. Outside this layer, the velocity distribution is uniform and is given by the inviscid velocity profile associated with the potential flow into a line sink. Thus, a marked contrast exists between the results for the converging flows and the corresponding results for high Reynolds numbers in diverging flow discussed earlier.

The above conclusions may be summarized qualitatively by reproducing the following passage from Goldstein[58]: "It appears that there is a very great difference between the cases of convergent and divergent flow. With increasing speed the velocity distribution, which at small Reynolds numbers and for small values of α is approximately parabolic, becomes, for convergent flow, flatter and flatter in the middle of the channel, the drop of the velocity to zero taking place in layers near the walls which become narrower as the Reynolds number is increased. For divergent flow, on the other hand, the velocity distribution alters with increasing Reynolds number in the opposite manner, the flux becoming more and more concentrated in the middle of the channel, until the Reynolds number is reached beyond which

purely divergent flow becomes impossible. When a larger outward flux than the critical one is forced through the channel, there are regions of backward flow."

Since the solution of the complete Navier-Stokes equations for the converging laminar flow has shown that at high Reynolds numbers, the effect of viscosity is significant only in the immediate vicinity of the walls, it would seem that the flow can be analyzed as though it were inviscid. Experimental evidence has confirmed the validity of this approach in both laminar and turbulent wall layers, provided the wall curvature is continuous and sustains no local adverse pressure gradient. Thus, the inviscid flow analysis has been particularly useful in the design of two-dimensional and axisymmetric contraction sections.

The steady, incompressible, inviscid two-dimensional flow between straight walls that converge can be analyzed using the methods of complex variables and conformal mapping (see e.g., Milne-Thomson[59]). This analysis shows that, although nowhere is there an area increase in the direction of flow, nevertheless two regions of adverse pressure distribution are seen to arise--one at the entrance to the convergent section and the other at the exit. While rounding off the sharp corners can mitigate this problem, adverse pressure gradients cannot be avoided in contractions of finite length. Since infinite contractions are impractical, there is a clear need to design profiles yielding a reasonable contraction length, without introducing excessively large adverse pressure gradients. The problem of axisymmetric contraction design has been approached by Cohen and Ritchie[60], based upon a generalization of the uniform cylindrical flow solution of the Stokes-Beltrami equation for the Stokes' stream function. They obtained a satisfactory wall profile and wall pressure gradient for a contraction with an area ratio of 7.4 to 1. Kachhara, et al.,[61] have investigated theoretically and experimentally contraction designs with a 4 to 1 area ratio. They solved the Stokes-Beltrami equation for finite contractions defined by the axial distribution of the wall slope and determined

that the nondimensional wall pressure gradient parameter $|1/(\rho U_2^2/2)| \times |dP_w/d(x/D_2)|$ can be as large as 0.38 before separation occurs. Here P_w is the wall pressure, x is the axial distance along the contraction and suffix 2 refers to conditions in the small diameter section downstream of the contraction.

So far we have considered laminar flows in contractions and expansions separately. Not much attention appears to have been devoted to single or multiple nozzle/diffuser combinations, except for the venturi tube whose design details as a flowmetering device can be found, for example, in Ward-Smith[49]. Of more direct interest to the UOTC concept is the recent work of Lee and Fung[62] which has examined the laminar flow in small blood vessels with constrictions. Steady, laminar flow in axisymmetric geometry is considered with a symmetric constriction defined by a bell-shaped curve according to the equation, $r/R = 1 - b \exp(-cz^2/R^2)$. Here r is the radial and z is the axial coordinate, R is the radius of the uniform tube away from the constriction, b is the amplitude of the local constriction ($b > 0$), and c is the sharpness factor. A larger value of c corresponds to a sharper profile, while a smaller value gives a flatter profile. Note that b and c are nondimensional. The constriction is roughly confined to the axial interval $-2R/\sqrt{c} < z < 2R/\sqrt{c}$, with the origin of the coordinate system being at the center of the constriction on the tube axis. For typical values of $b = 0.5$ and $c = 4$, the minimum diameter of the constriction is half the diameter of the tube and both the converging and diverging sections are each one tube radius long axially. This shows that the half angles of convergence and divergence are of the order of $\tan^{-1}(0.5) \approx 26.5°$. Lee and Fung have solved the Navier-Stokes equations numerically up to a Reynolds number of 25. They also performed experiments at higher Reynolds numbers and found that the flow remains laminar and the flow pattern is very similar to the theoretical predictions for Reynolds numbers up to 200. Their numerical results show that when the Reynolds number approaches zero, the flow is symmetric with respect to the center

of the constriction. At finite Reynolds numbers, the flow becomes asymmetric: for a profile defined by b = 0.5 and c = 4, a downstream eddy (i.e., on the diffuser side) appears when Re = 9.9. Below Re = 9.9, there is no eddy and when Re increases beyond 9.9, the point of separation starts moving upstream and the point of reattachment downstream. A more interesting result emerges from the examination of the axial distribution of the wall vorticity for three Reynolds numbers, viz., 1, 10, and 25. For the Hagen-Poiseuille velocity distribution in a tube (with no constriction), the dimensionless wall vorticity value is 2 and remains constant along the axial direction. With a constriction (b - 0.5, c = 4), however, the wall vorticity value has a highly peaked distribution. For Re = 1, the distribution is symmetric, with a peak value of wr occurring at the center of the constriction. At Re = 10 and Re = 25, the distributions become more asymmetric, the peaks (respectively equal to 29 and 36) shifting upstream. The wall vorticity values fall to 2 within one tube radius either side but at the two higher Reynolds numbers, the downstream wall vorticity values become negative over some axial distance. This indicates that flow reversal is occurring since the tangential shear stress at the wall in this region becomes negative (wall shear is proportional to the wall vorticity). Thus, the familiar Poiseuillean flow pattern is significantly affected by a local nonuniformity in the tube cross section. This is an interesting conclusion that is of relevance to UOT behavior. Although the work of Lee and Fung does not explicitly discuss the radial variation of velocity or vorticity fields, the streamlines computed at Re = 25 do reveal the tendency toward nonuniform radial profile of the axial velocity in the diffuser section.

In the long history of diffuser design and development turbulent flows have been far more extensively investigated than laminar flows with Reynolds numbers over 1,000 since the latter did not have much practical significance. We choose to discuss here some of the early works relating to the turbulent flow in diffusers but emphasize that this discussion is included less

for its relevance to UOTC and more for historical interest and for providing a starting point for our preliminary flow visualization studies.

Gibson[63] was one of the earliest investigators to comprehensively examine flows in diffusers. His experiments dealt with liquids, usually water in diffusers of different cross-sections, such as circular, rectangular, and square, and at different angles of divergence. He established that in turbulent-flow regimes the optimum included angle of divergence is of the order of 11° for rectangular cross section and in the range of 5°-8° for circular cross section. Apart from his early work on the uniformly diverging diffusers, Gibson's subsequent work considered trumpet-shaped diffusers and other types. Patterson[64] presented a thorough review of the literature up to 1938 on diffusing flows and discussed a wide variety of possible designs and configurations. Most of his discussions dealt with turbulent flows of liquids in diffusers of large dimensions. Ackeret[65,66], Sprenger[67], and Kline et al.[68], among others, performed a large number of experimental studies into the characteristics of straight and curved diffusers. A major finding of these investigations was that the thickness of the turbulent boundary layer at the diffuser inlet has a very strong influence on the efficiency of pressure recovery. Ackeret also applied the turbulent boundary-layer theory in successfully predicting the efficiency of a straight diffuser of circular cross section. Sprenger experimentally established the influence of the entrance length on the velocity distribution at the exit of the diffuser. He found that for small entrance lengths there is a "plateau" or core of uniform velocity at the exit and for longer lengths, the boundary layer reaches nearly to the center of the exit plane. Thus, in a diffuser of area ratio of 4 and total angle of divergence of 8° for a L/De = 0.85 (L and De are respectively the length and diameter of the entrance region), the exit velocity profile is uniform over the middle 45% of the exit diameter. This plateau region decreases to 30%, 20%, 10%, and 5% respectively for L/De

values of 2.85, 4.85, 6.85, and 8.85. Finally, at a value of 10.85, the flat profile at the center has nearly disappeared. These results are also given in Ackeret's review paper[65]. We note that the importance of keeping the length of the throat section in the UOT to a minimum has been emphasized previously.

Systematic calculations on turbulent boundary layers in straight diffusers of circular cross section were also carried out by Schlichting and Gersten[69]. Their results indicate the existence of an optimum total angle of divergence, 2α, for diffusers of equal area ratio and equal Reynolds number at entry. The optimum value is reckoned with respect to the maximum efficiency of pressure recovery. This optimum angle is found to lie between $2\alpha = 3°$ and $8°$ and to decrease with increasing entrance Reynolds numbers.

SECTION III

EXPERIMENTS WITH METAL TUBES

The easiest way to test the nozzle/diffuser configuration was to fabricate this particular geometry in a relatively long metal tube. Although such tubing would be an order of magnitude larger in bore diameter than a typical high-resolution gas chromatographic column, the behavior could be scaled accordingly. Previous experience using a variety of fabricated metal tubes convinced us that it would be possible to roll an appropriate geometry into a soft metal tube. Also we wanted to examine the flow properties of a simple segmented tube to determine the effect of regular constrictions on the permeability to gas flow as well as on solute band broadening.

1. Preparation of Metal Tube Test Specimens

Several different types of tubing material were considered for these experiments. Stainless steel, nickel, aluminum, and copper were examined with respect to ease of fabrication, i.e., forming the various UOT configurations. Eventually, it was decided to use copper tubing for the sequential concentric chamber tube (hereafter referred to as the segmented tube) as it could be easily worked with the special heat treated rolling tool designed for placing radial grooves in the tubing. Aluminum tubing was used for the UOT test specimen as it withstood the tapered rolling process better than copper.

Aluminum and copper tubing were originally obtained from Applied Science Laboratories of State College, Pennsylvania. Unmodified lengths of copper and aluminum tubing were cut to the finished length of 3.0 meters and served as "control" specimens. Also, as the Taylor-Golay equation would closely describe the dispersive behavior of these unmodified tubes, they would serve as comparison models. Specifically, the control aluminum tubing measured 3.0 meters by 2.1 mm ID and the control copper tube was 3.0 meters by 1.8 mm ID. The ends of these tubes

were deburred and the interiors flushed with acetone and eventually dried with a flow of nitrogen gas. The two control tubing sections were then sealed with plastic plugs and set aside awaiting further instrumental examinations.

A long section of copper tubing was processed by forming radially concentric constrictions at equal spacings (i.e., at 0.8 cm intervals) along the tube axis. A drawing of one of the three rollers that was used for forming these grooves (roller B) is shown in Figure 2. By maintaining a constant depth of penetration with the rolling device, the diameter of the constriction could be held relatively constant throughout the entire length of the tubing. This segmented tube was eventually cut to 3.0 meters in length and also subjected to an acetone flush and nitrogen drying prior to capping the ends. A similar fabrication procedure was followed for the aluminum UOT, only in this case special heat treated tapered rollers of the design shown in Figure 3 were used for forming the concentric converging/diverging undulated profiles along the tube axis.

A considerable amount of trial and error machining of the roller assembly was necessary before the desired UOT contour was obtained. Again, after the UOT test specimen had been cut to finished length, it was also cleaned with acetone, dried and capped. Over 100 manhours were required for the fabrication of these two modified specimen tubes. Also, there was a significant amount of preparation that preceded the actual rolling of the contours into the tubing. For example, light machine oil was found to be the best lubricating fluid for aiding the rolling of the grooves for the copper tubing; however, after trying a variety of lubricating agents, a liquid laundry detergent, Dawn®, was found to be the preferred lubricant for rolling the grooves into the aluminum tubing.

Photographs of cross-sections of tubular specimens generated by these two different rolling techniques are shown in Figure 4. Several interesting observations can be made from these

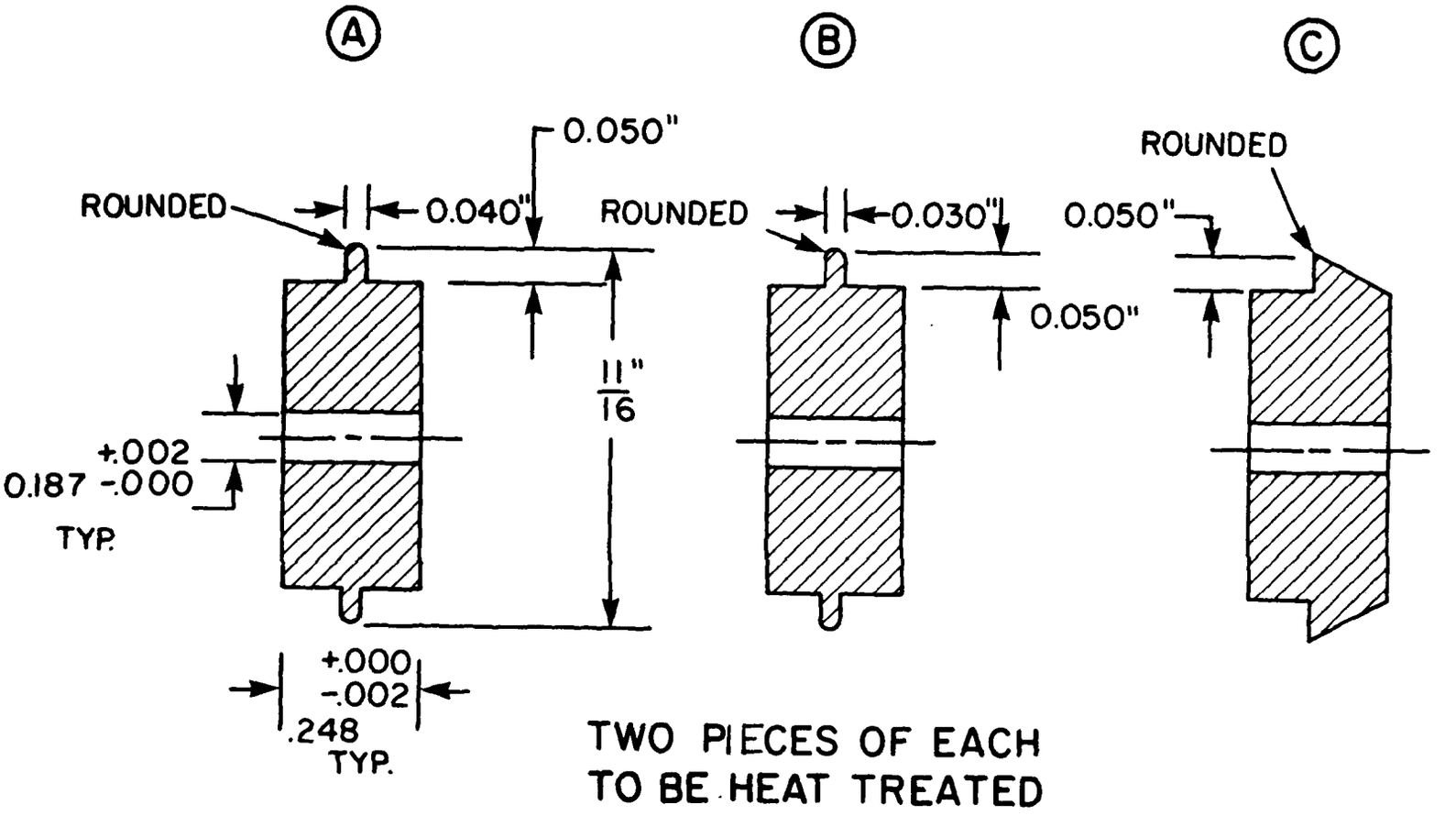

Figure 2. Typical roller for fabricating constrictions in segmented tube.

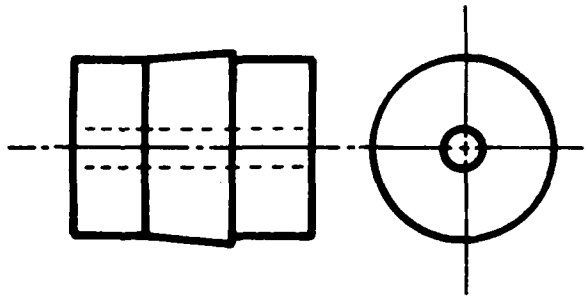

Dimensions are
in inches

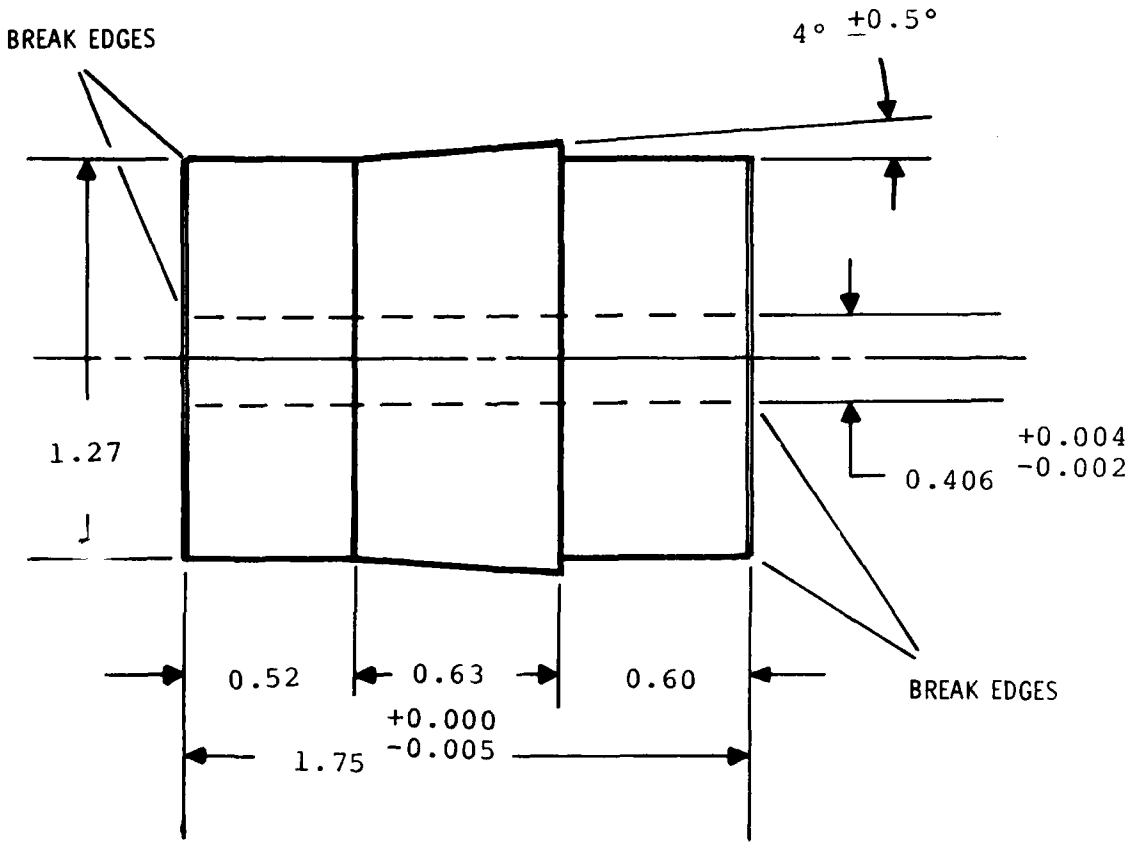

Figure 3. Typical roller for forming nozzle/diffuser configuration in aluminum tube.

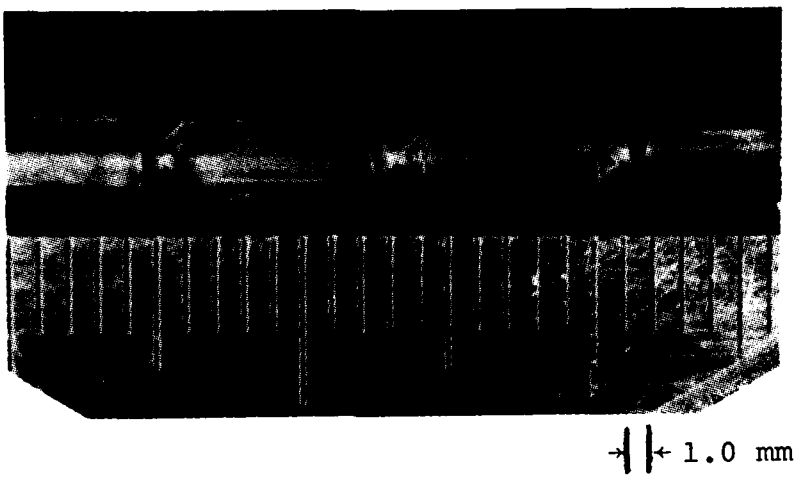

Copper Tube Section

Aluminum Tube Section

Figure 4. Cross-sections of formed tubular specimens.

photographs. We see that the copper segmented tube possesses sharp corners at the recesses both before and after the radial constriction. This flowpath geometry should produce some eddy mixing at these locations. The two separate sections of UOT tubing shown in Figure 5 are observed to be quite similar. Therefore, as these two particular test section samples represent UOT material that was prepared before and after the forming of the 3.0 meter aluminum test section, tool wear and associated variations in fabricating technique along the tubing length would seem to be minimal.

A series of preliminary examinations were conducted with the four tubing sections. (The actual experimental apparatus and procedure for these experiments will be described later in the report.) These initial examinations were disappointing and confusing. The zone dispersion behavior for the two uniform "control" tubes was as expected. However, the behavior of the copper segmented tube was quite confusing. Shortly after the segmented tube had been prepared, a tracer sample of methane was injected into the tube and with a helium carrier gas the zone spreading seemed to be as expected. However, several weeks later when a further test of the behavior of the copper segmented tube was conducted using a normal butane tracer in a nitrogen carrier, we found that it was difficult to transport the normal butane through the tube. The other confusing aspect of these early examinations was that the aluminum UOT test section seemed to produce the same dispersion behavior independent of whether the gas was flowing in the normal direction, that is, through the contraction section and then into the diffuser section, or whether the gas flowed in the opposite direction. It seemed to produce approximately the same degree of zone spreading behavior independent of flow direction. Also, in the original gas velocity regions that were examined, the UOT dispersion was considerably greater than that of the uniform unmodified cross-section aluminum tubing. Therefore, a detailed examination of several of the spare tubing sections was conducted.

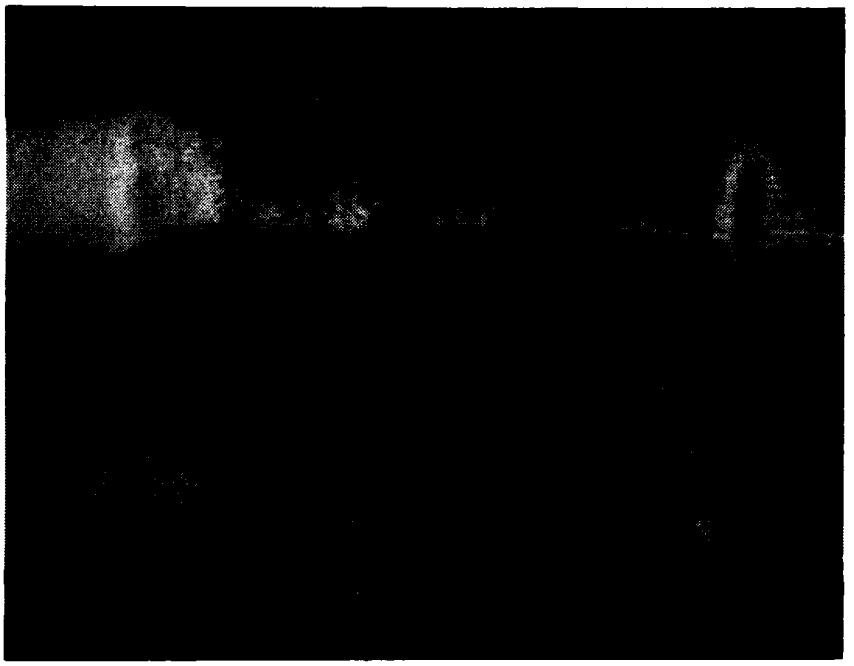

Figure 5. Magnified view of aluminum UOT interior.

Figure 5 shows a magnified photographic view of the aluminum UOT interior and we see that modified region of the surface appears to be pitted and relatively rough. This tubing specimen was then examined with the use of a scanning electron microscope and images at 350X and 1200X are shown in Figure 6. Indeed we now see a very rough interior, one which seems to have the appearance of scales or platelets. Consequently, from what is known with respect to the effects of wall roughness relative to fluid flow behavior, the surface roughness of these modified tubes could have a pronounced effect upon the gas transport, and associated dispersion, for both the copper segmented tube and the aluminum UOT section. Also, this form of surface roughness could be functioning as a retentive mechanism in much the same manner as molecular sieves retard migrating solute zones in gas chromatography. In addition to the surface roughness, there was some question about the chemical cleanliness and possible adsorptivity of these surfaces. Accordingly, it was decided that a very thorough cleaning was necessary for the interior surfaces of each of the metal tube specimens. A dilute solution of phosphoric acid (0.87 M) was selected as the primary cleaning agent for the aluminum tubing while a dilute solution of nitric acid (1.1 M) was used for the copper tubing.

Each of the two copper tubes, that is the "control" tube and the segmented tube, was cleaned in the following manner: Approximately 50 ml of distilled water was passed through the tube, followed by the dilute solution of nitric acid, and then a 50 ml water rinse. After purging with nitrogen gas, 50 ml quantities of each of acetone, methylene chloride, and acetone were passed through the tube in sequence. Finally the tube interior was dried with a stream of flowing nitrogen gas. The ends of the cleaned tubing section were then sealed with clean plastic caps. The same procedure was followed for the two aluminum test sections, only the dilute solution of phosphoric acid was substituted for the nitric acid. These newly cleaned test sections were then examined systematically using the experimental test procedure as diagrammed in Figure 7.

350X

1200X

Figure 6. SEM images of UOT inner surfaces.

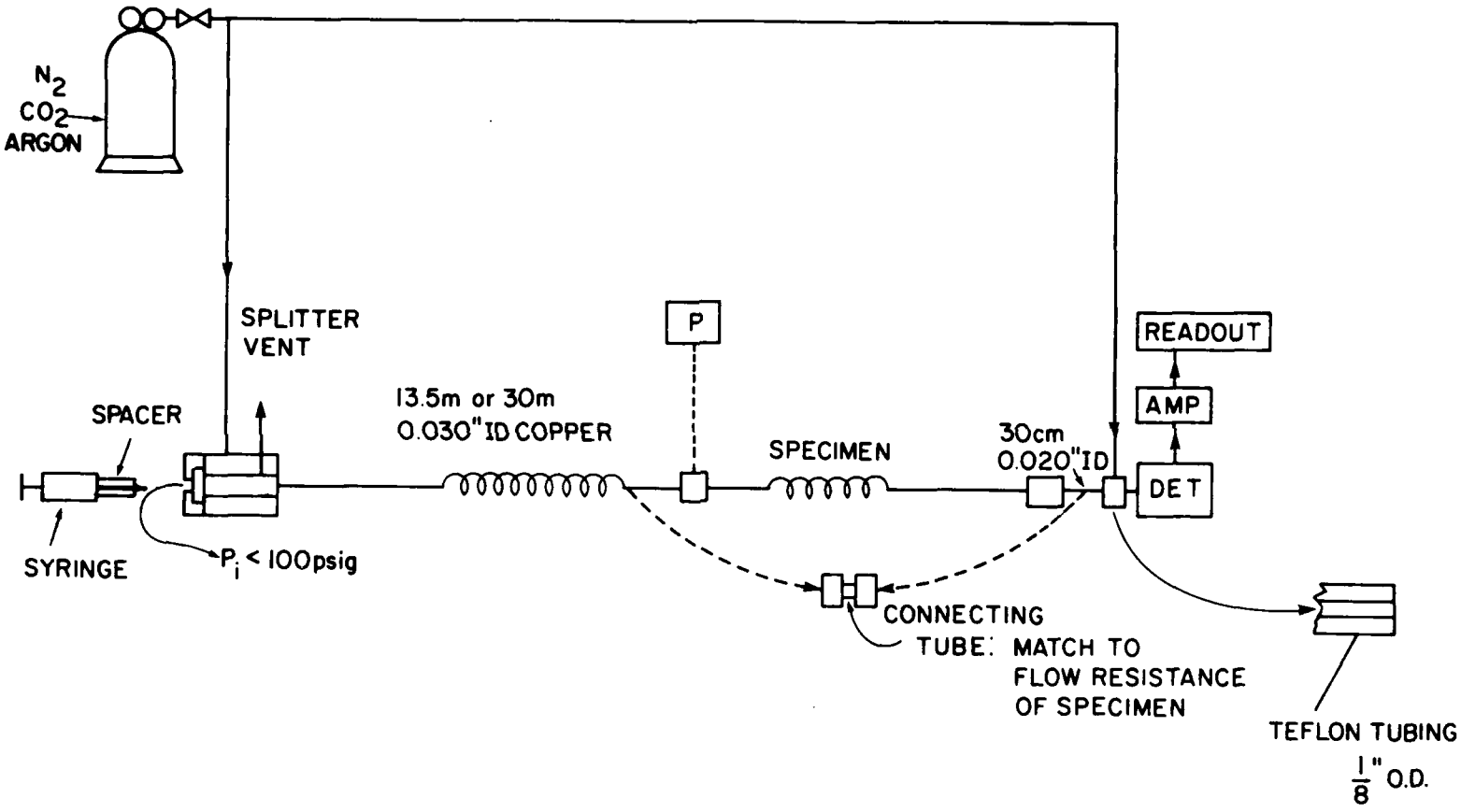

Figure 7. Schematic of experimental dispersion test system.

From the previous observations of the surface roughness of the copper segmented tube and the aluminum UOT test section, there was still some concern about surface roughness and absorptive surface effects with these modified tubes. Therefore, several polymeric solutions were considered for the coating of the inner surfaces of these tube sections. Some thought was given to the dimethylsilicones such as the SE-30 silicone gum. Also, the various polyethylene glycol polymers were considered. Initially, the Carbowax 1000 seemed to be a suitable candidate for coating the interior of these tubes. However, a material was needed that would be crystalline in nature at room temperature. Therefore, we selected a higher molecular weight of polyethylene glycol, specifically the Carbowax 20 M material. This particular polymer is also used as a gas chromatographic stationary phase in separation columns. The particular sample that we selected was indeed material that was intended for the preparation of chromatographic columns.

Five grams of Carbowax 20 M was dissolved in 100 ml of methylene chloride. Approximately 2 ml of this solution was forced through each of the four tubular test sections. This was accomplished at room temperature and the tube was immediately dried in a stream of nitrogen gas. The dispersive behaviors of these coated metal tubes were then experimentally examined in exactly the same manner as the previous series of dispersion tests.

2. Measurement of Dispersion Properties

The dispersive properties of a long narrow bore tubular section can be evaluated by using a tracer pulse technique. Specifically, if a concentrated pulse of a suitable chemical tracer is injected into a linear tubular system which includes a sensitive and rapid response detection system, the gas phase spreading or dispersion for the entire system can be established. If one of the major components of this in-line system is the

tubular test section in question, then its dispersive behavior can be isolated.

For a series arrangement of independent dispersion devices, the bandwidth variances of each are additive. Specifically, the distribution variance for the tracer injection process plus the individual variances associated with the inlet tubing member, the tubular test specimen, and the entire detection process are all additive. If one determines the sum of these variances when the test member is absent from the system, and then determines the total variance when the test member is included in the system, the band spreading variance due to the tubular test specimen is the difference between these two values.

In this experimental procedure, nitrogen was selected as the carrier gas and normal butane was selected as the tracer substance. The diffusion coefficient of normal butane in nitrogen seemed appropriate for our experimental test procedure. The more common combination of a methane tracer in helium would have produced an efficiency versus carrier gas velocity curve that would have been difficult to measure with the limited 3.0 meter length of our test sections. In the lower velocity regions of the dispersion experiments, a Houston 5000 series potentiometric strip chart recorder was used for recording the response profiles. However, at higher linear gas velocities (those exceeding approximately 0.75 meters per second) a galvanometric system had to be employed to measure the rapidly changing electrical signals resulting from the normal butane elution profile. For these measurements, a Brush Model 260 galvanometric system was employed and chart advances were at speeds up to 25 mm/sec. This system showed the capability of following a 50 Hertz signal. These dispersion measurements were carried out using a modified Varian 1800 Series gas chromatograph. Specially modified injection ports and detector assemblies were utilized so that dead volumes and unswept regions were minimized. Highly diluted samples of normal butane in air (100 ppm) were injected into the modified injection port using a Precision Sampling Corporation Pressure-Lok syringe. These injections (20 microliters) were made by

the same operator and were accomplished in less than approximately 0.1 second. The photographs of the sample injection components are shown in Figure 8, and the chromatograph with its high-speed galvanometric recorder is presented in Figure 9. The various tubular test specimens are shown in Figure 10. The timing of events was accomplished using stopwatches and the calibrated timed chart advances of the recording systems. Pressures were measured using the instrument pressure gage on the Varian 1800 gas chromatograph and a Hamilton No. 86805 septum piercing pressure gage. Due to the very dilute samples used in these experiments, signal attenuations were varied to obtain recorded peaks of approximately the same height. The recorded peak heights varied at most by a factor of two. Thus, any errors associated with peak width measurements would be normalized as the peak profiles were somewhat similar.

The graphic data resulting from these experiments was processed using a light box, an optical magnifier with built-in reticle, or in some cases, a simple metal metric rule was employed for measuring the peak widths at half height. From these measurements the variances of the emerging zone profiles could be calculated. For each test condition the zone variance corresponding to the entire gas flowpath system was compared with the variance when the flowpath did not contain the tubular test specimen. The data for these series of experiments are presented in Tables 4 through 8 and the corresponding dispersion versus linear gas velocity profiles are presented in Figures 11, 12, and 13.

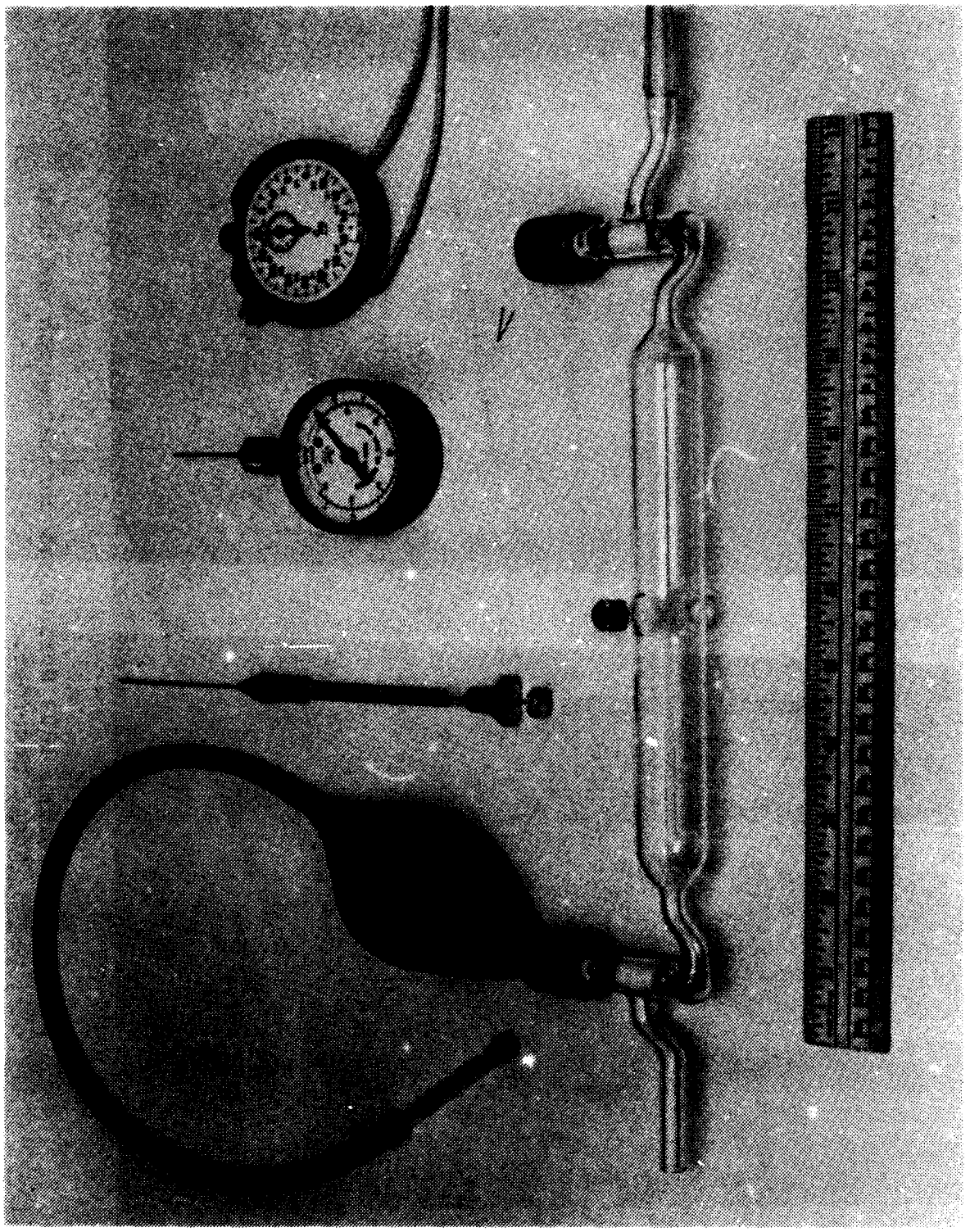

Figure 8. Photograph of sample injection components.

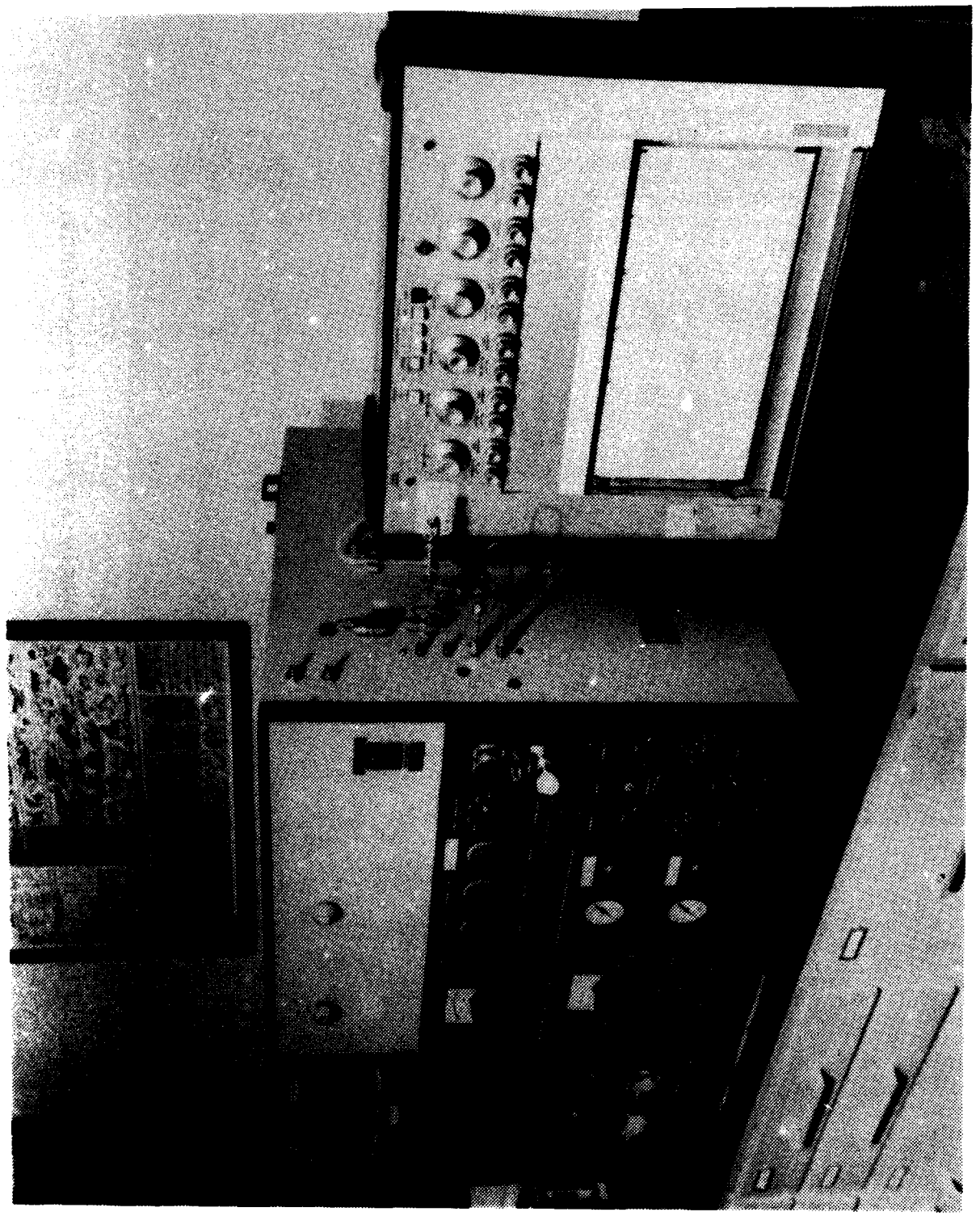

Figure 9. Varian 1800 Series gas chromatograph and high speed recorder.

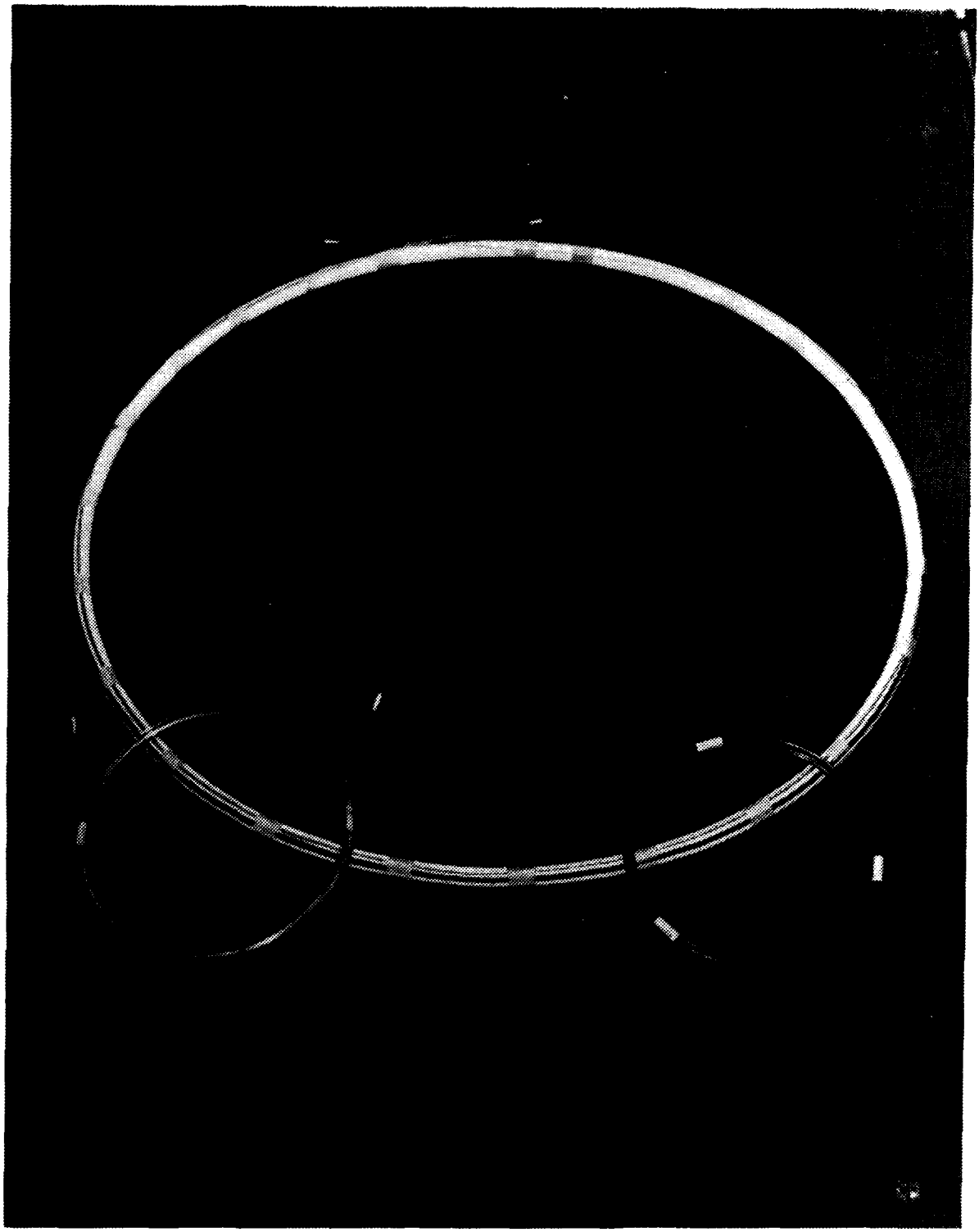

Figure 10. The various metal tubular specimens.

TABLE 4

DISPERSION DATA FOR UNCOATED ALUMINUM
UNDULATED OPEN TUBE (UOT)

(Flow in Reverse Direction)

Linear Carrier Gas Velocity ($\bar{v}$, $cm \cdot sec^{-1}$)	Height Equivalent to a Theoretical Plate ($\bar{H}$, mm)
6.58	0.577
6.70	0.612
8.36	0.642
8.36	0.661
12.24	0.652
12.35	0.629
18.13	1.135
18.93	1.168
28.6	1.654
29.7	1.788
59.3	3.61
60.0	3.26
133.9	10.06
135.1	9.81
238.0	17.37
241.0	19.20

TABLE 5

DISPERSION DATA FOR COATED ALUMINUM UOT

(Flow in Original Direction)

Linear Carrier Gas Velocity ($\bar{v}$, $cm \cdot sec^{-1}$)	Height Equivalent to a Theoretical Plate ($\bar{H}$, mm)
4.01	1.000
4.05	1.041
6.29	1.007
6.33	1.003
11.95	0.747
11.58	0.671
16.95	0.952
16.39	0.942
31.3	1.960
30.6	1.880
58.4	3.49
57.9	2.95
153.1	11.92
140.2	12.78
291.0	24.3
261.0	18.0

TABLE 6

DISPERSION DATA FOR COATED ALUMINUM UOT

(Flow in Reverse Direction)

Linear Carrier Gas Velocity ($\bar{v}$, $cm \cdot sec^{-1}$)	Height Equivalent to a Theoretical Plate ($\bar{H}$, mm)
4.09	1.052
4.03	0.979
6.33	0.729
6.42	0.782
11.86	0.736
12.00	0.688
16.30	0.931
16.85	1.050
31.6	2.16
30.9	1.92
58.6	3.32
58.8	3.86
144.2	12.52
163.0	16.65

TABLE 7

DISPERSION DATA FOR COATED CYLINDRICAL ALUMINUM TUBE

Linear Carrier Gas Velocity ($\bar{v}$, $cm \cdot sec^{-1}$)	Height Equivalent to a Theoretical Plate ($\bar{H}$, mm)
3.24	0.948
3.23	1.009
5.39	0.714
5.30	0.691
9.90	0.700
10.00	0.764
14.15	0.943
13.64	0.914
27.5	1.520
26.6	1.414
48.9	2.16
49.2	2.63
123.0	7.34
121.0	5.46
216.0	14.3
204.0	12.8

TABLE 8

DISPERSION DATA FOR COATED CYLINDRICAL COPPER TUBE

Linear Carrier Gas Velocity ($\bar{v}$, $cm \cdot sec^{-1}$)	Height Equivalent to a Theoretical Plate ($\bar{H}$, mm)
3.76	0.828
3.78	0.830
6.28	0.970
6.16	0.918
11.81	0.667
11.81	0.627
16.30	0.882
16.04	0.902
30.6	1.599
31.9	1.891
58.5	2.51
57.9	3.04
163.0	6.51
164.8	7.80
261.0	13.8
256.0	10.6

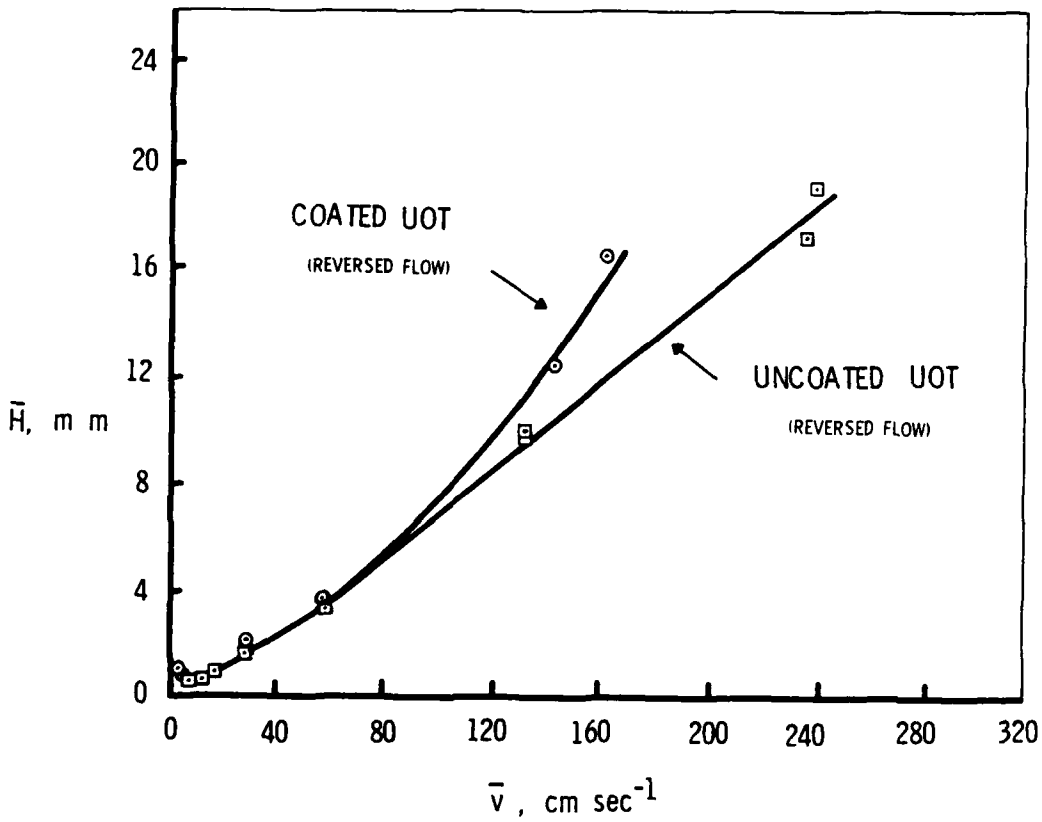

Figure 11. Dispersion versus velocity plots for the aluminum UOT with reversed gas flow.

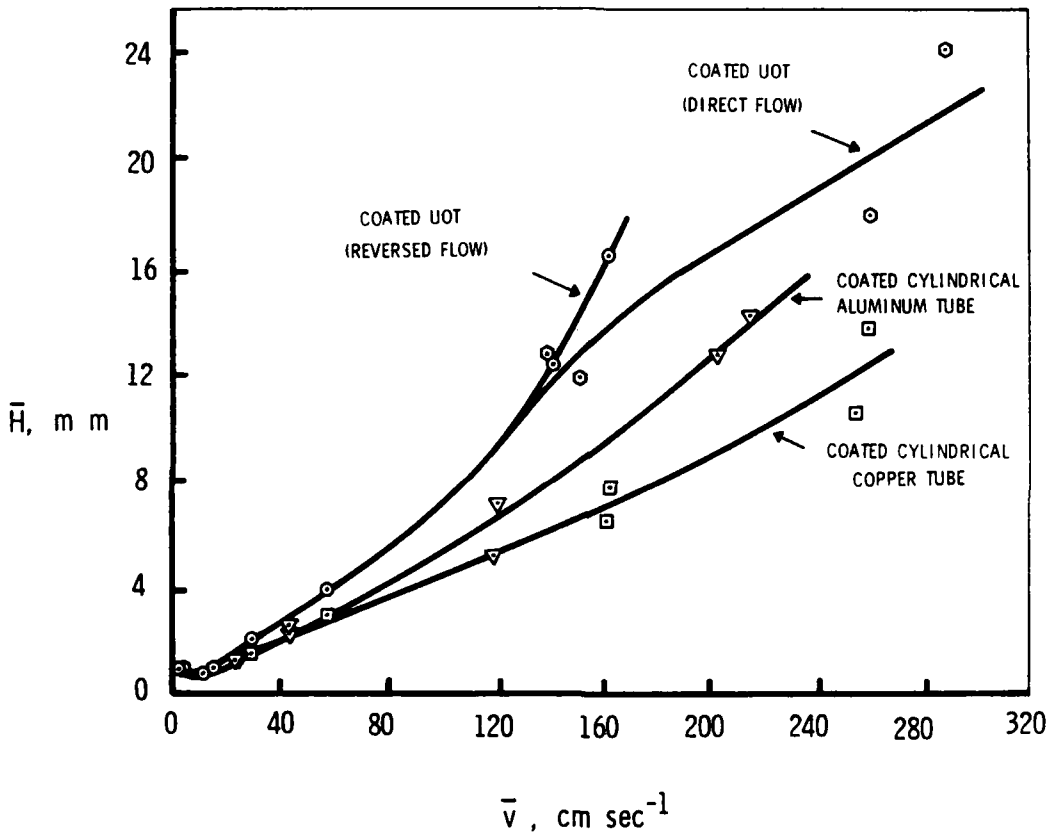

Figure 12. Dispersion versus velocity profiles for the various coated tubular specimens.

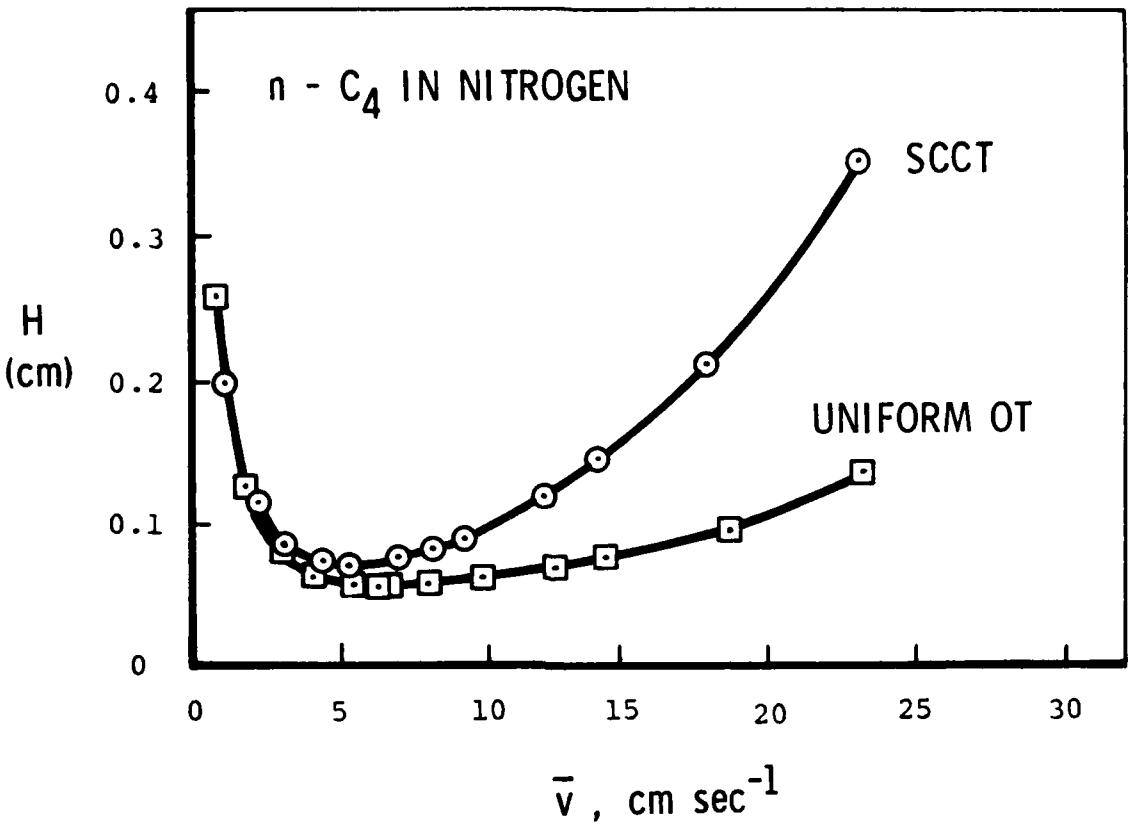

UNIFORM COPPER OT		SEGMENTED COATED COPPER TUBE SCCT	
$\bar{v}$ (cm·sec^{-1})	H (cm)	$\bar{v}$ (cm·sec^{-1})	H (cm)
0.88	0.258	1.221	0.1967
1.90	0.126	2.273	0.1143
3.07	0.0780	3.343	0.0824
4.27	0.0627	4.56	0.0713
5.79	0.0575	5.44	0.0685
6.49	0.0553	7.12	0.0745
6.91	0.0554	8.33	0.0802
8.30	0.0575	9.49	0.0879
10.04	0.0611	12.2	0.1193
12.6	0.0679	14.0	0.1430
14.3	0.0749	17.9	0.2113
18.7	0.0952	23.1	0.3503
23.3	0.1355		

Figure 13. Data from segmented tube experiments.

SECTION IV

FLOW VISUALIZATION EXPERIMENTS

The brief review presented in Section II has described the available fluid dynamic information that is of some relevance to the understanding of the flowfield in an undulated open tube. It has been noted, however, that this information is neither complete nor adequate to provide a rational approach to the design of an UOTC. Two approaches exist for obtaining the desired information. The first approach involves the analytical examination of the UOT through the numerical solution of the Navier-Stokes equations. Here, a parametric study of different wall profiles, and of different angles of convergence and divergence could be conducted, in a manner analogous to that of Lee and and Fung[62], to yield the optimum UOT configuration. In the second approach, a somewhat more qualitative understanding is generated from experiments that yield information on the flow pattern and velocity profiles through flow visualization. In a configuration like the UOT, where the optimization involves several variables, both these approaches must be considered as complementary to each other. Furthermore, a visual examination of the flowfield and qualitative understanding therof would be useful before a comprehensive theoretical study is carried out. Accordingly, it was decided that during the first phase of this research program, attention would be given to the flow visualization aspects in a representative UOT configuration.

Visual observation is often the first step in the elucidation and understanding of many physical phenomena. This is especially true of the motion of fluids. From the very beginning experimental fluid mechanics has relied upon flow visualization to observe and survey the relevant parts of a flowfield, and thereby to facilitate the understanding of the physics of the flow problem. A well known example is the experimental investigation of Osborne Reynolds in 1879 who studied laminar-to-turbulent transition in a horizontal circular tube by observing the

behavior of a dye injected into a water flow. A variety of techniques for flow visualization have become established and been employed not only in experimental fluid mechanics but also in other technical disciplines. Although visualization has been primarily a qualitative research tool, many techniques have been developed that can also yield quantitative information on a flowfield. Thus, visualization techniques are available for the observation and measurement of (i) a streak line, a path line, and a stream line, all of which show the flow direction and flow pattern, (ii) distributions of flow velocity, its gradient, and acceleration, (iii) vortices, their generation and decay, laminar-to-turbulent transitions, and separation and reattachment of a flow, and (iv) distributions of density and temperature of a fluid.

In the UOT configuration we are interested in obtaining the flow pattern and the velocity profiles at different salient axial stations. In the steady laminar flow, the stream line, the streak line, and the particle path all coincide and a visual representation of the stream lines gives the flow pattern. A knowledge of the flow pattern is helpful in the optimization of the configuration. For instance, presence of boundary-layer separation and consequent recirculating eddying motion in the diffuser would suggest that for the flow Reynolds number under consideration, the angle of divergence is too large. A knowledge of the velocity profile shows clearly the extent to which the axial velocity is uniform in the radial direction at different axial locations of the configuration. An additional insight that comes from the flow visualization relates to the extent of radial dispersion of a tracer that is injected into the main stream. The latter information is particularly useful in the evaluation of the UOT as a chromatographic column.

Before we discuss further the suitable techniques of flow visualization that are applicable to the UOT configuration, it is necessary to examine certain similitude considerations. We have mentioned earlier that a representative UOT configuration has an

internal diameter of the order of 1 mm. For the flow of gases like hydrogen and helium at a velocity of the order of 1 m/s that is typical of gas chromatography, the flow Reynolds number is of the order of 10. Clearly, the flow visualization also must be performed at Reynolds numbers that are of this order, if the visualization results are to have any relevance to the flowfield behavior of the UOT. It is also obvious that it is extremely difficult to perform and difficult to interpret the flow visualization in flow paths that are of the order of 1 mm in width. Furthermore, it is impossible to introduce any probe or injector of finite dimensions in order to render the flow visible for visual inspection or photographic record. Even if the introduction of a small probe in a 1 mm tube were possible experimentally, the very presence of such a probe would cause flowfield disturbances that are much larger than the characteristic flowfield variations in the UOT that are under investigation in the first place. While this leads to the inescapable conclusion that the flow visualization must be performed only in scaled-up models of the UOT configuration, the question remains as to how relevant a scaled-up model would be to the actual UOT behavior.

The answer to the above question is provided by the well known similarity considerations of fluid dynamics. We are justified in the results obtained from the visualization of the flow in a model (scaled-up in our case) to the UOT prototype only if the flowfield behavior is similar in the two systems. By similarity we mean the similarity of motion or the kinematic similarity. When the two flowfields are kinematically similar, their streamline patterns are similar. The necessary condition for the kinematic similarity in the two systems is that they be geometrically similar. Clearly, the fully established laminar flows in two circular tubes satisfy the geometrical similarity requirement easily. However, when the flow is not fully established, i.e., when another length scale, in addition to the tube diameter, is involved, the two circular tubes need not be geometrically similar. This becomes clear if we consider a very long slender tube and a very short fat tube. The two circular tubes are geometrically similar if and only if the length-to-diameter ratio

is the same in both tubes. Thus, between the scaled-up flow visualization model and the UOT prototype, we need to preserve the same values of the length-to-diameter ratio in all the corresponding sections such as the entrance to the convergence, convergence throat, divergence, and exit of divergence. Also, the contraction and expansion ratios must remain the same in both the systems. These requirements would imply that the two systems would have equal values of the angle of convergence and angle of divergence. Therefore, once a UOT path is specified, a geometrically similar visualization model is established, except for the scale of magnification. The latter is determined subject to the experimental constraints relating to the availability of space, and flow rate capability of a reservoir of fluid used in visualization experiments.

Geometrical similarity between the two systems alone is insufficient to ensure that the two flowfields are similar. When effects such as buoyancy, heat, and mass transfer are unimportant, the sufficient condition for steady, incompressible flows is provided by the dynamic similarity requirement that the Reynolds number in both systems must be the same. Needless to say, the two Reynolds numbers are correctly defined with respect to the corresponding length and velocity scales. Thus, we must specify for both systems identical Reynolds numbers based upon identical locations, such as the entrance to the convergence or the throat or the exit of the divergence. We recall that the definition of Reynolds number involves, in addition to the length and velocity scales, two other parameters which relate to the properties of a fluid, viz., the mass density and absolute viscosity (the kinematic viscosity is the ratio of the absolute viscosity and mass density). Thus, in addition to the length and velocity scales which essentially determine the scale of magnification between the UOT prototype and flow visualization model, the fluid employed in the visualization experiment is also left to the choice of the experimentalist, as long as the

Reynolds numbers at a particular condition are the same in the model and the prototype.

The foregoing discussion is of immense help in the design of a suitable flow visualization scheme. First, geometrical similarity consideration allows us to employ a scaled-up model for flow visualization which avoids any flowfield distortions associated with the introduction of probes of finite size in small-diameter tubes. Second, due to dynamical similarity arguments, the flowfield behavior of a gas in the UOT configuration can be examined more easily by flow visualization in liquids. Unlike gas flows, liquid flows can be visualized through several relatively simple techniques. Also, the availability of inexpensive water-soluble polymers makes it possible to obtain any desired kinematic viscosity. With the appropriate choice of viscosity, the visualization experiment could be conducted at low enough viscosities which can be obtained in relatively simple laboratory apparatus.

In view of these considerations, it was decided to prepare scaled-up models for flow visualization in aqueous solutions of polymers. Although visualization is easier to perform and interpret in two-dimensional (i.e., planar) flow configurations, it was decided at the outset to conduct the testing directly in axisymmetric geometry (circular cross-section). This was based on the rationale that the optimum shape (e.g., the angle of divergence) in the axisymmetric geometry is not likely to be the same as in the two-dimensional geometry. It may be recalled that this is indeed the case for turbulent flow in diffusers discussed in Section II. Another aspect relating to the geometrical similarity deserves mention here. For complete geometrical similarity, apart from the similarity of the overall shape between the model and the prototype, it is essential that the surface roughness in both systems must also be geometrically similar! It is clear that this requirement is not always easy to attain. Since the eventual chromatographic column based on the UOT configuration will be in glass (coated with the appropriate stationary phase) of fairly

smooth walls (this precludes, at least initially, the presence of surface whiskers), the scaled-up models were built in glass. It also turned out that drawing the desired shape out of glass tubes was easier and less expensive than other forming techniques applied to other materials such as plexiglas.

A schematic of the initial scaled-up model is shown in Figure 14. A total included angle used (2α) for the diffuser was 7°. The diameter upstream of the nozzle and downstream of the diffuser was 50 mm and the throat diameter was 25 mm. Thus, the contraction and expansion area ratios are both equal to 4. The straight sections ahead of the contraction and following the diffuser were one diameter long (50 mm). There was no significant straight section at the throat since a smooth rounding off merged the throat both upstream and downstream. Similar rounding off was resorted to upstream of the nozzle and downstream of the diffuser. Since the laminar flow is more tolerant of a contraction (too rapid a contraction, of course, can cause separation), the design of this section was not deemed to be critical. Smooth rounded wall profile was obtained directly as a result of glass blowing. Thus, the area reduction in the nozzle takes place over a distance of one initial diameter. On the other hand, the use of 7° for the angle of divergence necessitated a diffuser length of 200 mm or about 8 (initial) diameters. Also, this section has essentially a linear wall taper and required a specially designed and constructed stainless steel mandrel. It is this aspect that precluded the fabrication of a number of visualization models of different shapes and angles of divergence. Accordingly, the research effort was directed to the refining of the flow visualization aspects and thereby establishing the flow patterns and velocity profiles in one specific configuration. The question of obtaining optimum configuration for the typical Reynolds numbers of interest was not addressed.

From the dimensions of the model, it is clear that this represents a scale of magnification of 50 to 1 with respect to a UOT configuration of 1 mm initial diameter. That the overall

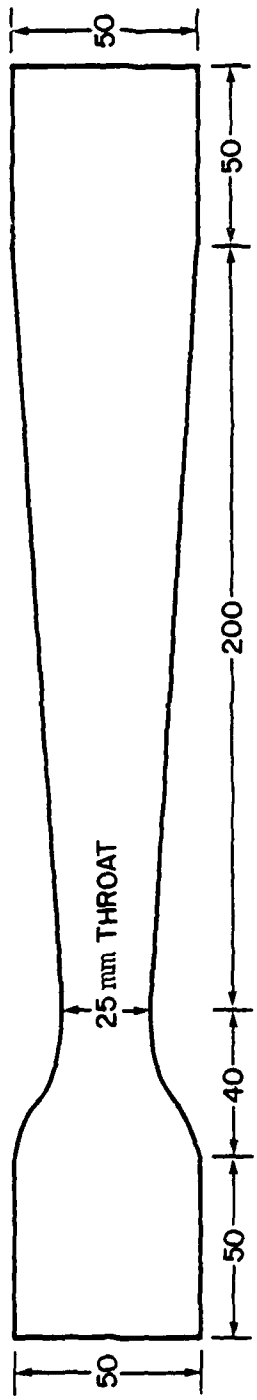

DIMENSIONS ARE IN MILLIMETERS

Figure 14. Schematic of initial scaled-up model.

length of the model is of the order of 35 cm clearly indicates that unlike the hundreds of nozzle/diffuser elements in the UOTC, only a very small number of scaled-up models could be held in series for flow visualization in the laboratory. In fact, three models for the one design under consideration were built. Flow visualization was performed with a single model or with two of them in a series. Also, preliminary experimentation to test the apparatus and refine the visualization techniques was done with a straight circular tube (of length-to-diameter ratio of 24) alone and with that tube followed by one model. The latter arrangement wherein the fully-established parabolic velocity gets established in the straight circular tube meant that at the entrance to the convergent section the velocity profile was parabolic. This configuration then represented the most stringent test of the performance of the UOT with respect to its ability to modify the initial parabolic profile into a more uniform profile. A less stringent arrangement involved the elimination of the straight tube. Instead, the UOT model was preceded by a short bell-shaped entry section of 4 to 1 contraction ratio. This assured a nearly uniform velocity profile at the entrance of the convergent section.

It has been seen that based upon a 1 mm diameter tube and 1 m/s mean gas flow velocity, the Reynolds number for hydrogen or helium is about 10. Therefore, it is possible to estimate the velocity and flowrate requirements in the flow visualization model under consideration. Thus, for an entrance Reynolds number of 10 (based upon the diameter of 49 mm), the ratio of the mean velocity to the kinematic viscosity must be equal to $10/4.9$ cm^{-1}. We note that at a temperature of 20°C, the kinematic viscosity of water is approximately 1 cs = 1×10^{-2} cm^2/s. Therefore, the use of pure water in the model would imply that the mean flow velocity is of the order of 2×10^{-2} cm/s. Obviously, this is too small a velocity of flow for buoyancy effects to become insignificant. However, it should not be surprising that dynamic similarity considerations imply such a low water velocity. In

going from gas flow in the UOT prototype to water flow in the visualization model, our length scale is increased by a factor of 50 while the kinematic viscosity scale has decreased by a factor of 100. Hence, the velocity scale must decrease by a factor of 5,000 (i.e., from 1 m/s gas velocity to 2×10^{-2} cm/s water velocity). This is precisely where the availability of water-soluble polymers becomes extremely helpful.

A survey of the easily available and relatively inexpensive water-soluble polymers showed that the polyethylene glycols are among the most suitable candidates for visualization tests. These polymers, marketed by Union Carbide Corporation under the trade name "CARBOWAX", are available at different molecular weights. As the molecular weight of the polymer increases, the viscosity of its aqueous solution increases. Thus, for instance, the aqueous solution of the polymer at 25% by weight has a kinematic viscosity at 25°C ranging from 2.2 cs to 820 cs in the polymer molecular weight range of 200 through 20,000. The available viscosity range compares very well with that of castor oil (680 cs), glycerine (750 cs), or SAE 250 gear oil (1,300 cs) in pure form. Clearly, the oils are far less desirable in terms of experimental convenience, and environmental acceptability. Moreover, it was found that the polymer solution in water was far less expensive than castor oil, for example, to give the same kinematic viscosity. Among the polymers, CARBOWAX 20M (of 20,000 molecular weight) was selected for the flow visualization experiment. The use of 25% by weight aqueous solution of 20M with a kinematic viscosity of 820 cs (more than 800 times that of pure water) indicates that a Reynolds number of 10 in the model (which is 50 times larger than the prototype) is easily obtained with a mean flow velocity of the order of 16 cm/s--a velocity large enough to eliminate the free convective effects and small enough to be obtained with just gravity head in a small tank. It is also easy to see that higher Reynolds numbers in the range of 100-1,000 can be obtained in such a system without a commensurate increase in the mean flow velocity by using aqueous solution of 20M in concentrations lower than 25% by weight. For example, at the mean flow velocities

of 16 cm/s, polymer solutions having the kinematic viscosities of 8 cs and 80 cs respectively yield Reynolds number of 100 and 1,000 based on the initial diameter of the model.

The schematic of the experimental system for flow visualization is seen in Figure 15. The apparatus consists of a 30-gallon tank (2' x 1 1/2' x 1 1/2') which has the main reservoir feeding the aqueous solution of the polymer through a bell-shaped entrance (of 4 to 1 contraction ratio) into the test section. This tank is provided with an overflow in order to assure a constant liquid head for the liquid flow through the test section. The height of the overflow device can be varied to give a liquid head from a minimum of a few centimeters to a maximum of 36 cm above the centerline of the flowpath. We note that a gravity head of 30 cm can give an efflux velocity of 2.4 m/s when no loss due to frictional effects is considered. Due to viscous friction in the flowpath, the available head is reduced and the actual velocity is less than the maximum. But this feed system has no difficulty giving velocities of the order of 10 cm/s. Indeed, additional pressure drop is required to ensure that the flow velocities are of this order. A downstream contraction (of about 16 to 1 area ratio) and a valve cause the required pressure drop for attaining flow velocities of the desired range.

The test section is made up of one or two UOT models or of a straight tube followed by one UOT model. Downstream of the test section is a collection tank of 11-1/2 gallon capacity. A small centrifugal pump is used to deliver the liquid from the collection tank to an overhead-supply tank. Liquid flow from this tank into the main tank can be controlled so as to keep the level therein constant. Thus, the visualization system is a closed-circuit loop, and avoids wastage and frequent replenishment of the polymer solution. However, when the visualization scheme involves the use of a dye, the entire liquids must be discarded after several experimental runs, since the increase in background color would begin to reduce the contrast between the main stream and the injected dye.

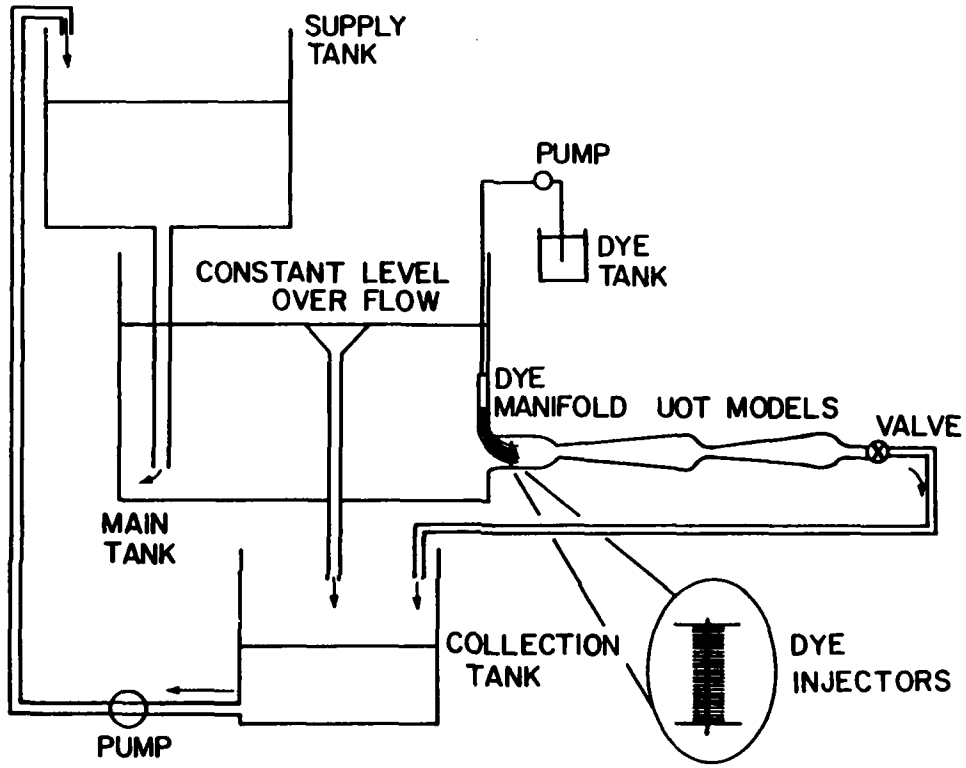

Figure 15. Schematic of flow visualization system.

Several techniques are available for visualizing the motion of a liquid. After a review of the literature, three techniques were considered suitable in the present UOT flow visualization experiments. These are the dye injection method, hydrogen-bubble technique, and electrolyte dye production (or tellurium dye method). Detailed discussion of these three techniques is available in a number of references[70-72]. A brief description of these techniques is given here.

The injection of dye has long been a popular method of introducing discrete tracer filaments into a fluid stream. In steady flow, the dye traces the streamline which provides a visual indication of the flow pattern. Both continuous and pulse injection of the dye are possible but the pulsing is generally not accurate enough to yield direct measurements of velocity. The major disadvantage in this method is the disturbance to the flowfield caused by the introduction of the dye injectors. Since the injection velocity of the dye filament must be equal to the velocity of the surrounding stream, the design of the injection system is critical.

The hydrogen-bubble technique involves electrolysis of water. Bubbles of hydrogen at the cathode or of oxygen at the anode, swept from the electrodes by the flowing liquid, may be used as tracers. Since the volume of hydrogen produced is twice that of the oxygen, attention is usually given to hydrogen bubbles. It is attractive to use these electroytically generated gas bubbles for flow visualization, since the number and size of the bubbles may be regulated by adjusting the voltage. The bubbles may be shed from a wire cathode in the form of a cloud, filament, or sheet. A fine platinum wire of 0.001 in. in diameter, when placed normal to the mean flow direction, generates a row of bubbles along the wire with a short electric pulse. These bubbles are shed off the wire, carried away with the flow, and deformed according to the local velocity profile. Repetitive pulses produce successive rows of bubbles, which mark in the flow curves separated by a constant flow time. The drawback

in this method is the buoyancy effect whereby the hydrogen bubbles rise in the flow during their motion with the liquid. It is essential to have bubbles of very small size so that their rise rate is kept as low as possible.

In the third technique, tracer particles are generated in the fluid electrochemically. The use of a tellurium wire as a cathode in water is a good example. When a potential is applied to the wire, particles of elemental tellurium and oxygen are released. The tellurium particles are swept from the wire as a black colloidal cloud which could be easily photographed. This technique suffers from the fragility of tellurium wire which is rapidly made worse by the electrochemical process itself.

Present flow visualization experiments investigated the dye injection method and hydrogen bubble technique. The tellurium-dye method was not tried in view of the limited time.

A great deal of the effort has been spent in refining the dye injection system. Several injector schemes were tried before the successful system was in place. This system consists of a thin rake placed vertically in the flowpath (immediately downstream of the bell-shaped entrance section). This rake supports twenty very fine hypodermic needles (0.305 mm I.D. and 0.559 mm O.D.) which are placed horizontally at 2.4 mm center-to-center distance. Thus, this arrangement provides twenty dye filaments spanning the cross section of the test section. All these injection tubes are connected to an inlet manifold through fine teflon tubings. A gear pump is employed to feed the manifold with the dye solution from a reservoir. Preliminary experiments have employed a red fluorescent dye which is made to fluoresce under the illumination from an ultraviolet lamp.

SECTION V

GLASS TUBE FABRICATION PROCEDURES

At the present time, the best material for the preparation of HRGC columns is glass or fused silica. Accordingly, to prepare very high performance HRGC columns of UOT construction, it would be necessary to develop techniques for fabricating these geometries out of glass tubing.

In the past we have prepared numerous HRGC columns using glass tubing that was drawn on a Shimadzu GDM-1 glass drawing machine. Previous work in glass surface chemistry and glass surface modification[73-75] for the improvement of HRGC columns was then utilized. The present work involved modification of the Shimadzu GDM-1 for making these undulated open tubes out of glass.

Initially several possible techniques for producing glass UOT's were discussed. These include applying a precisely pulsed heat source (i.e., lasers, spot heater, etc.) while drawing the glass tubing (stretching the glass into the precise form desired), pulsing a three jaw graphitized collet while the glass is intermittently advanced through the drawing machine, or using small heated rollers to form the glass undulated open tubes. It was decided that the feasibility of each of these processes or combinations of them should be evaluated. One of the processes would then be chosen and a prototype constructed.

The use of a laser was an appealing idea because of the speed with which it could be pulsed. As with the spot heaters, it was realized that the area heated would be extremely small in relation to the glass size. Therefore, many lasers or spot heaters would be required to heat the glass circumferentially. This would be expensive as well as space consuming. However, these ideas would probably be applicable for use with fused silica tubing. Because fused silica tubing is drawn at speeds greater than one meter/second, the use of a laser would be desirable because of the fast pulse rate that can be obtained with a laser.

The three jaw graphitized collet had merits for this project because it could maintain a circular cross-section in the formed glass which was an essential requirement of the task. Upon further examination, it was realized that graphite forms with precise dimensions on the order of less than 1 mm would be difficult to machine. Another drawback was overcoming the cracking of the glass due to mechanical shock. To reduce mechanical shock the three forms would have to be squeezed around the glass rather than pushed with arms. In order to squeeze the glass, the drawing process would have to be stopped long enough for the squeezing action to take place. Experimentally, it was determined that the drawing process could be stopped for intervals of up to ten seconds with no change in the finished tubing size or shape.

The final process evaluated and eventually pursued involved the use of two heated rollers that were located 180° apart which were graphite coated.

The original configuration of the Shimadzu GDM-1 glass drawing machine can be seen in Figure 16. In order to obtain an undulated form in drawn tubing, several modifications had to be made. For undulated glass tubing not to be deformed while coiling, a large diameter coiling tube was made. This coiling tube was formed using 0.25 inch O.D. by 0.180 inch I.D. with 24 inch length general purpose (18-8) stainless steel. A length of 4.5 inches on one end was kept straight while the remainder was wrapped around a mandrel (6.5 inch diameter). Connections were made for the power source, and the tube was mounted and coated with a graphite spray. Soft glass tubing (7 mm O.D. by 5 mm I.D.) was then drawn at a draw ratio of 25, yielding finished tubing with an outer diameter of 1.2 mm. A length of tubing greater than ten meters was then drawn successfully. The finished coils had a diameter of 175 mm.

The next step involved designing and building a prototype unit with spring tension on the rollers to mount on the glass drawing machine (see Figures 17a thru 17d). This unit was designed so that a gear drive mechanism could be added in the

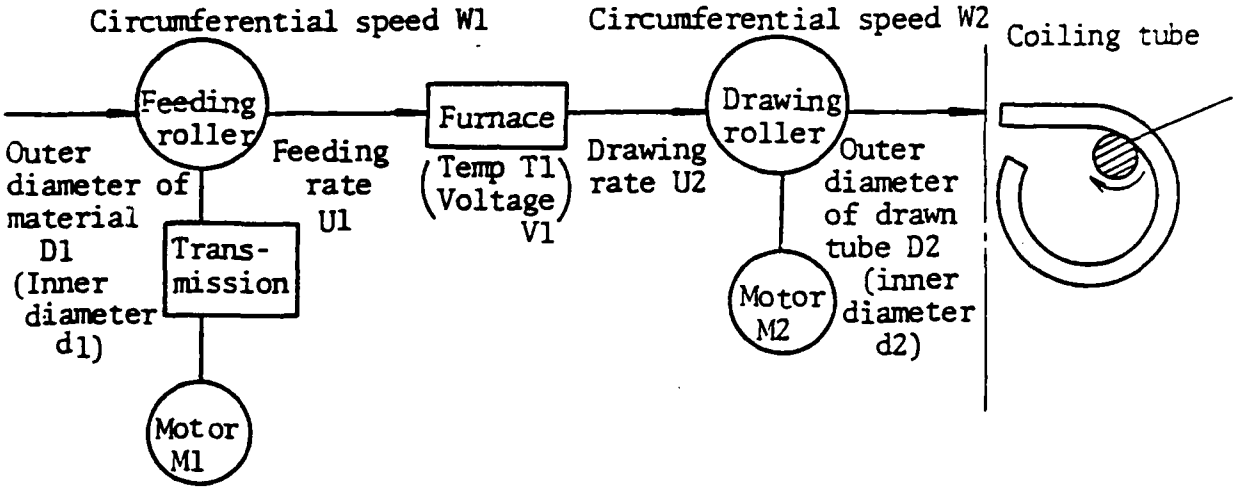

Figure 16. Functional schematic of Shimadzu GDM-1 glass drawing machine.

(a) Mounting Block for Heated Rollers

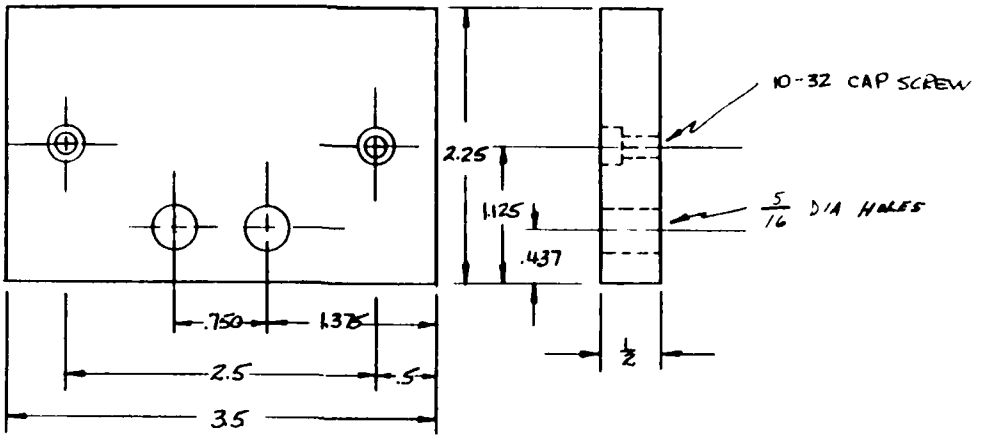

(b) Mounting Brackets for Alum. Block

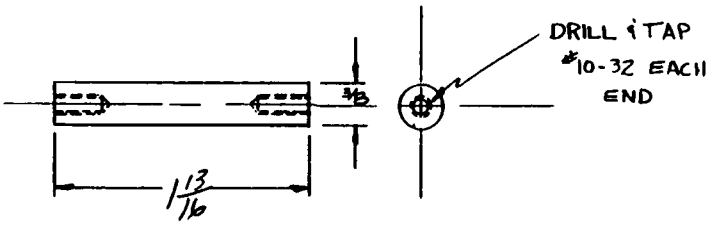

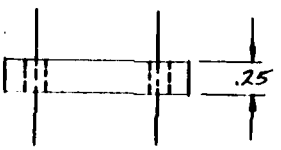

(c) Lever Arms for Heated Rollers

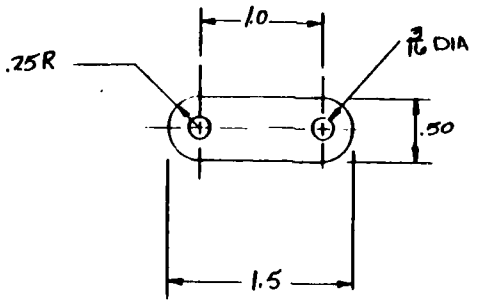

(d) Prototype of Forming Rollers

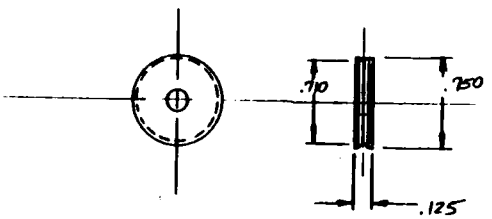

Figure 17. Fabricated parts for modifying the glass drawing machine.

future. The initial rollers were designed simply to see if the glass could be formed by this process. The unit was mounted on the glass drawing machine between the furnace and drawing roller (see Figure 16).

Previous experience with the glass drawing machine showed that the drawn glass tubing was cooled below the melting point of the glass before leaving the furnace. Therefore, an auxillary heat source was required before the glass can be formed by rollers. Initially a small heating coil was formed from furnace wire which was powered by a 20 ampere, 5 volt power source. This furnace was capable of high temperatures, but the glass either cooled down before the rollers could form it or else the furnace would be so hot as to melt the glass to the point of dripping. Because of these problems, the heated coil was abandoned and replaced with the use of a heat gun. The heat gun had the disadvantage of spreading heat to too wide a region, which adversely affected the drawing rollers. A small propane-oxygen flame was then used by aiming it at the rollers. It was then noticed that a tremendous amount of heat was being drawn away from the rollers through conduction. Therefore, the centers of the rollers were reamed out and replaced by transite.

With the above modifications to the glass drawing machine, glass tubing could be drawn and successfully reformed by the rollers. However, soft glass often cracked at the rollers because of thermal shock. The glass used in later trials was Pyrex (borosilicate) because it is less susceptible to thermal shock. After determining that the glass could be formed with rollers, two small gears were made from a long piece of brass gear stock. These gears were fitted with a transite center so as to reduce heat conduction from the rollers. A "V" shaped groove 0.7 mm wide and 0.7 mm deep was cut into the gears so that they would form the glass and still maintain a circular cross-section.

If the glass temperature can be maintained at the forming temperature, the circular cross-section of the glass should be maintained. However, if the temperature is too high, the glass will melt and conform to the V shape which would be a disadvantage. It was then decided to use two flames for heating. Each flame was located 180° apart and 90° from the plane of the gears. This heating technique was abandoned, however, because of the lack of good control over the amount of heat present.

Glass pieces, however, were drawn through the gear arrangement with a single flame heat source. Several short sections of capillary tubing which had been crinkled were obtained. Visual inspection of the finished tubing indicated that the cross-section had remained circular throughout. Examples of the finished product can be seen in the photograph presented in Figure 18. It should be noted that although the outer diameter has been altered, the inner diameter remained constant. This occurred because the groove in the gears was larger than the inner diameter. If larger tubing were drawn, the inner diameter would also be undulated. In order to make UOT's which would be useable for chromatographic evaluation, three additions to the current system would have to be made.

The first addition would be a spot heater whereby there could be some variation in the amount of heat delivered. This would allow greater control of the heating of the glass and thus would permit greater uniformity in the undulating process. Secondly, the undulating gears must be driven in a synchronized manner so that circular cross-section is maintained. This could be accomplished either by the use of a gear system or possibly by the use of belts driven by the synchronous motor which currently drives the drawing rollers. The third addition would involve the modification of the undulated gears to produce the optimized design of the UOT.

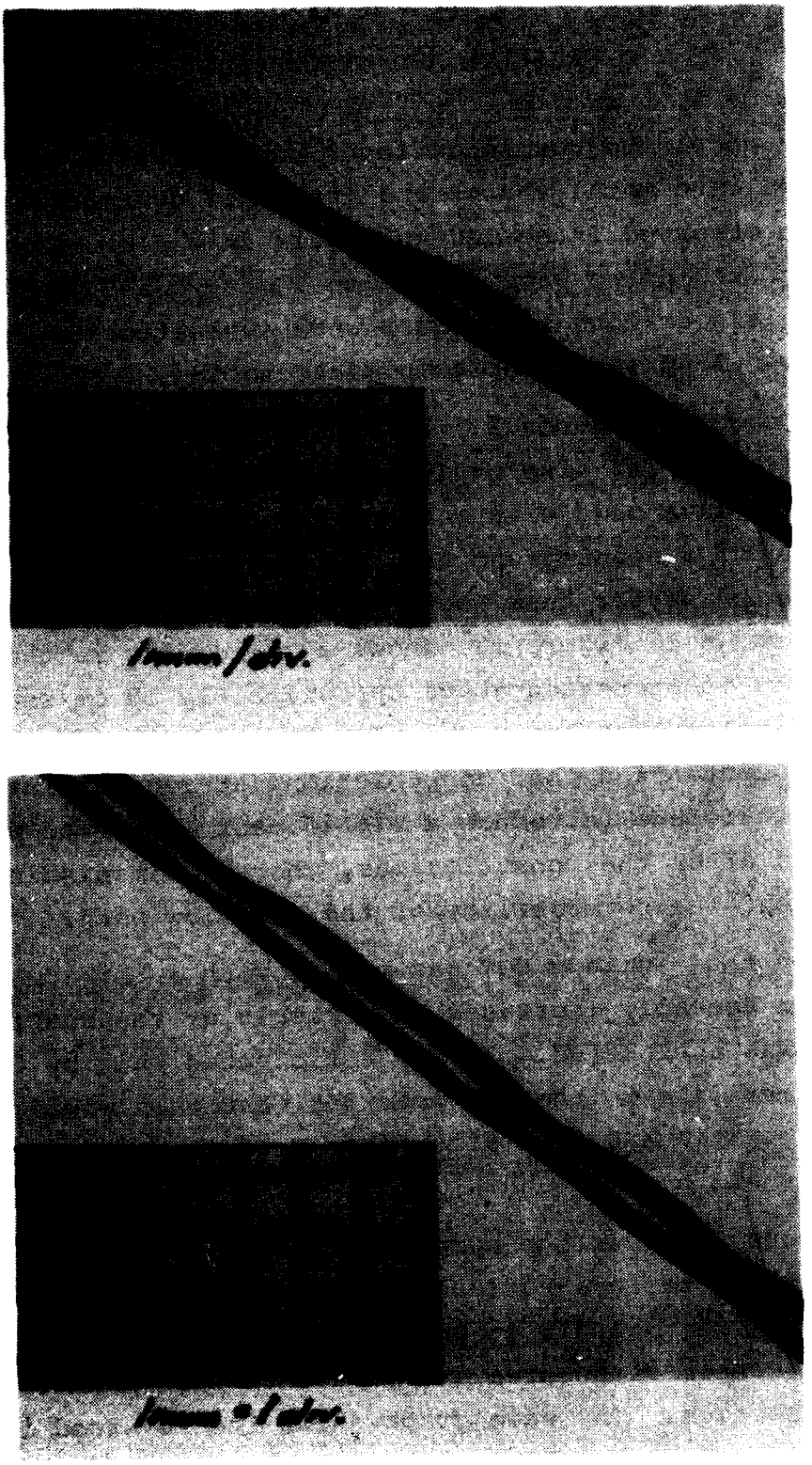

Figure 18. Undulated Glass Tubing.

SECTION VI

RESULTS AND DISCUSSION

The undulated nozzle/diffuser configuration has been fabricated into metal shapes and its fluid dynamic behavior has also been observed in scaled-up models in a flow visualization test apparatus using water and tracer materials. In addition, special glass drawing techniques were evaluated for forming undulated cylindrical shapes in glass tubing.

As seen in Figures 11, 12, and 13 the nozzle/diffuser undulated shape and also the segmented cylindrical tubing offer no distinct advantage with respect to producing less gas-phase dispersion of a solute zone as it passes through the tubing length. The segmented copper tube when compared to a cylindrical copper tube, as shown in Figure 13, shows a rapid rise in the dispersion as velocity is increased above approximately 10 cm/sec. Also, this particular tube had a considerable resistance to gas flow. It is our contention that constrictions at regular intervals in a cylindrical tube introduce a significant amount of mixing both before and after the constrictions, thereby diminishing to a very large extent the permeability of the gas flow path.

When the aluminum UOT was coated with a thin polymer film, dispersion actually increased as a result of the coating process, and this was unexpected. It was anticipated that by applying a thin polymer film to the UOT interior that this would mask absorptive sites and also fill in some of the surface distortions, pits, or small cracks.

Figure 12 shows the comparison between the cylindrical aluminum tube, the cylindrical copper tube, and the UOT, with flow in the original direction, i.e., for gas flowing through the sharp constriction area and then into the gradually tapered diffuser section. The same graph shows the reversed flow situation where gas is actually entering into the diffuser section first and then flowing into the throat region.

As expected, the copper tube shows a lower dispersion than the aluminum tube. This is reasonable as the copper tube has a somewhat smaller bore. However, the coated UOT tube shows much greater dispersion at the higher linear gas velocities and this is especially striking since the mean diameter of the coated UOT would be much smaller than the coated aluminum tubing and also somewhat smaller than the coated copper tube. So it is quite evident that the UOT tube, both in the direct flow direction and in the reverse flow direction, introduces a greater degree of dispersion to a tracer zone than does an equivalent cylindrical bore tube.

A small section of the aluminum UOT tube has been sacrificed, and there did not appear to be any flaking of polymeric coating that could have presented flow disturbances. Also, the constrictions seemed to be concentric with the maximum diameter of the tubing interior.

Thus, with the interior of this coated UOT being intact and as the diffuser included angle is such that flow separation should not occur, then it would appear that the favorable modification of the velocity profile that occurs in the constriction portion of the nozzle/diffuser arrangement is negated, and even surpassed, by the undesirable velocity profile modification that occurs in the diffuser section. Therefore, it can be concluded that for laminar gas flow, the resultant dispersion for a given length of undulated open tubing was found to be greater than that for an equivalent mean diameter cylindrical bore tube.

As noted in Section IV, our flow visualization studies examined the dye injection system and the hydrogen bubble technique. In the former, several injection systems were evaluated for their suitability. Although only the system eventually adopted is described in Section IV, preliminary experiments investigated simpler arrangements but the results were not satisfactory. For example, the dye issued out of fine holes pierced along a narrow-bore teflon tube which was aligned

normal to the mean flow direction. The orientation and uniformity of such holes in a teflon tube left much to be desired. Significant improvement in the size and alignment of the holes resulted when the teflon tubing was replaced by a fine stainless steel tube. The drilling of over 20 small holes equally spaced along the length of the thin stainless steel tube was, of course, an exacting task. Such an injection system, however, suffered from another problem. With both gravity feed and pump feed of the dye, the holes farther away from the dye reservoir tended to issue lesser amounts of dye into the mainstream. Also, the injection velocity could not be kept the same. These factors resulted in much poorer and distorted flow patterns.

The evolution of the final injection system occurred toward the end of the research program. Thus, only a demonstration of the feasibility of the method to the UOT model evaluation could be carried out. Because of the use of twenty parallel dye filaments pump fed from an inlet filament, the earlier shortcomings due to nonuniform injection rate and injection velocity were eliminated. The success with this dye-injection arrangement can be seen in Figure 19 which illustrates the streamline pattern obtained in the UOT model. Although the quality of the photograph could be improved, it is clear from the picture that the UOT model yields flow pattern that shows the anticipated trend. Unlike in a straight circular tube wherein the laminar flow under the flow Reynolds number considered gives rise to the parabolic velocity profile, the UOT model tends toward a more uniform velocity profile. Furthermore, one observes that the flow pattern in the UOT model is very smooth and that the flow in the diffuser section is free from separation and recirculation. Additional investigations with both single and multiple UOT elements would have been instructive.

It is useful to mention here one feature of the dye-injection method of visualization that was noticed both in direct observation and in the photographs. Unless extreme care was exercised in eliminating disturbance in the main tank (see Figure 20), a nonzero swirl velocity component was present at the bell-shaped

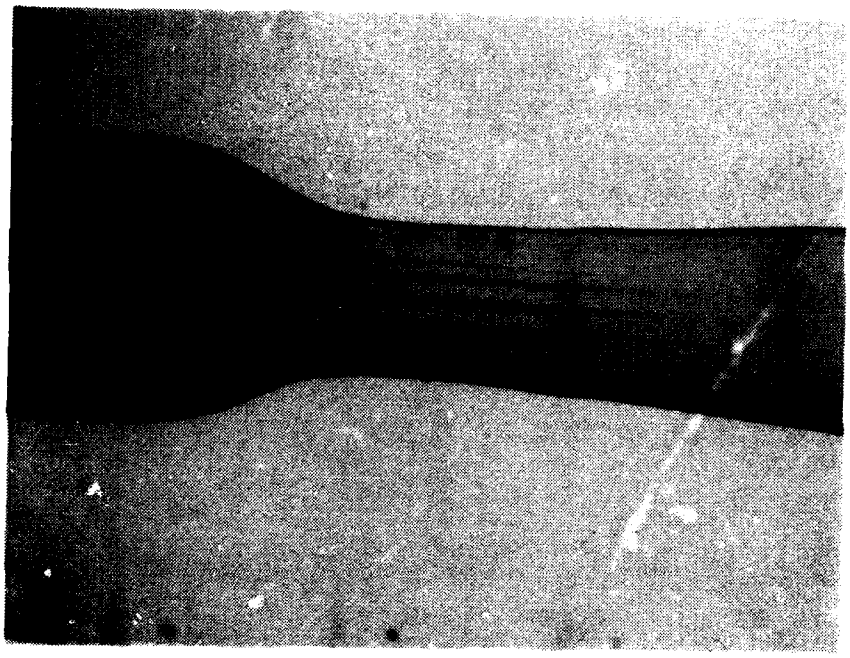

Figure 19. Photograph of streamline pattern.

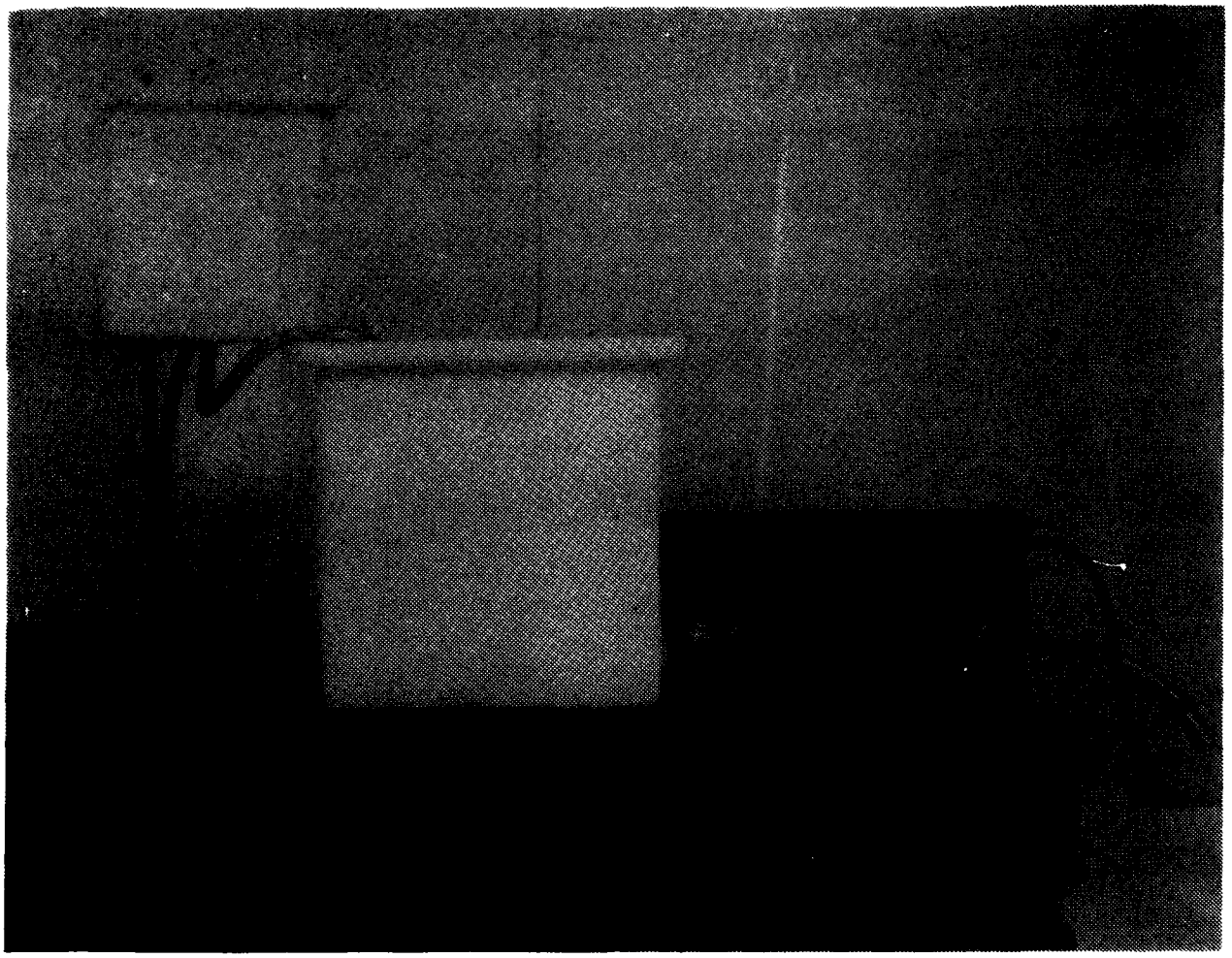

Figure 20. Apparatus for Flow Visualization Studies.

entrance to the test section. This caused a slow turning of the streamline pattern and a still picture was a time-averaged representation over the exposure time. Indeed, the somewhat broadened dye filment in the contraction section of the UOT model seen in Figure 19 is indicative of the swirling motion.

Before we settled on the above-mentioned dye-injection system, our flow visualization experiments also considered the hydrogen-bubble technique. These early experiments did establish the applicability of this technique for the UOT work. However, at the main stream velocities considered, the buoyant motion of hydrogen bubbles was a serious problem. The bubbles rapidly rose to the top half of the UOT model and defeated the value of this technique. Figure 21 illustrates this problem. Further parametric examination of different main stream velocities, bubble size (which depends on both the size of the platinum wire and applied voltage) and rate of production of bubbles was necessary before an optimum combination for minimal buoyant effects could be determined. This was not done during the present research. We believe, however, that both the hydrogen-bubble technique and the tellurium-dye method deserve further consideration, especially in view of their potential for giving quantitative information on the velocity profile.

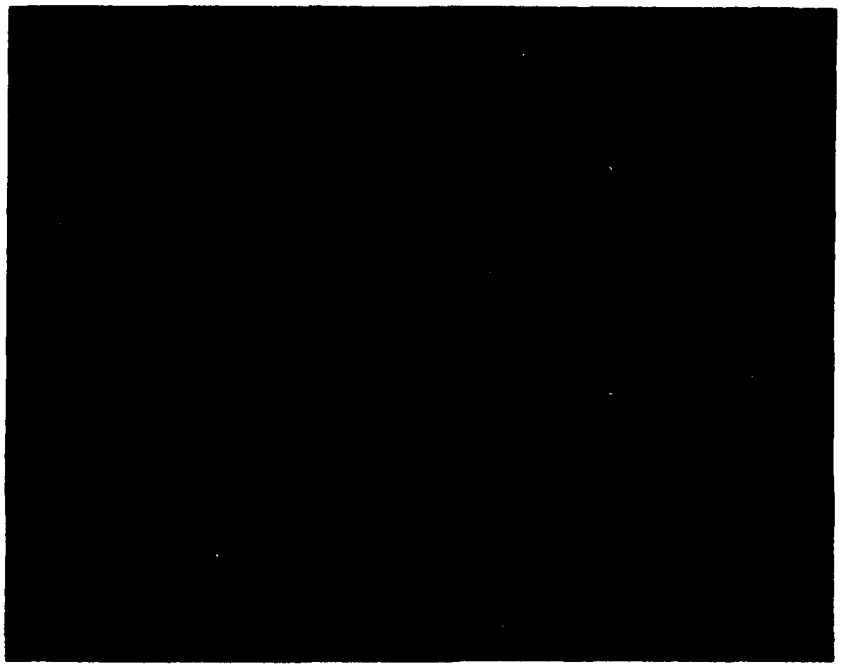

Figure 21. Photograph of Buoyancy Effects in Hydrogen-Bubble Technique.

SECTION VII

CONCLUSIONS

The behavior of flowing liquids and gases in an undulated open tubular flowpath was investigated. Undulated metal tubes of a nozzle/diffuser configuration can be made, however this is a very slow, time-consuming process. It was also demonstrated in this study that undulated glass tubes can apparently be processed using present technology, although the smaller bore diameter tubes would be difficult to fabricate.

From the theoretical examinations and experiments conducted with simple nozzle/diffuser undulated tubes, gas zone dispersion was greater than that for smooth cylindrical tubing of uniform cross section. Although this study focused on a relatively narrow range of mass flow rates and fluid densities, it would appear that in the laminar flow regime, dispersion is minimized with a uniform cylindrical tube of constant circular cross-section.

REFERENCES

1. Roeraade, J., Some Aspects of High-Resolution Glass Capillary: Preparation Criteria, Possibilities, and Limitations, Chromatographia, 8(9), 511, 1975.

2. Schomburg, G., Practical Limitations of Capillary Gas Chromatography, J. High Res. Chromatog., 2, 461, 1979.

3. Golay, M. J. E., Theory of Chromatography in Open and Coated Tubular Columns with Round and Rectangular Cross-Section, Gas Chromatography 1958, Ed., D. H. Desty, Butterworths, London, p. 36, 1958.

4. Golay, M. J. E., Height Equivalent to a Theoretical Plate of an Open Tubular Column Lined with a Porous Layer, Anal. Chem., 40, 382, 1968.

5. Desty, D. H., The Origination, Development, and Potentialities of Glass Capillary Columns, Chromatographia, 8, 452, 1975.

6. Desty, D. H. and Douglas, A. A., Non-Circular Capillary Columns for Gas Chromatography, J. Chromatog., 142, 39, 1977.

7. Popendick, H. D. and Baudisch, J., Tapeworm Columns in Gas Chromatography, J. Chromatog., 122, 443, 1976.

8. Golay, M. J. E., Gas Chromatography with Open Tubular Columns - Past and Present, Paper presented at American Chemical Society Meeting in Atlanta, March 1981.

9. Everett, D. H. and Haynes, J. M., Model Studies of Capillary Condensation: Cylindrical Pore Model with Zero Contact Angle, J. Coll. Interface Sci., 38, 125, 1972.

10. VanDeemter, J. J., Zinderweg, F. J., and Klinkenberg, A., Longitudinal Diffusion and Resistance to Mass Transfer as Causes of Nonideality in Chromatography, Chem. Eng. Sci., 5, 271, 1956.

11. Littlewood, A. B., An Examination of Column Efficiency in Gas-Liquid Chromatography Using Columns of Wetted Glass Beads, Gas Chromatography 1958, Ed. D. H. Desty, Academic Press, New York, p. 23, 1958.

12. Golay, M. J. E., Vapor Phase Chromatography and the Telegrapher's Equation, Anal. Chem., 29, 928, 1957.

13. Golay, M. J. E., Theory and Practice of Gas Liquid Partition Chromatography with Coated Capillaries, Gas Chromatography 1958, Ed. V. J. Coates, Academic Press, New York, p. 1, 1958.

14. Ettre, L., Purcell, J., and Norem, S., Support-Coated Open Tubular Columns, J. Gas Chrom., 3, 181, 1965.

15. Taylor, G. I., Dispersion of Soluble Matter in Solvent Flowing Slowly Through a Tube, Proc. Ray. Soc., A219, 186, 1953.

16. Aris, R., On the Dispersion of a Solute in a Fluid Flowing Through a Tube, Proc. Ray. Soc., A235, 67, 1956.

17. Halasz, I. and Heine, E., Packed Capillary Columns in Gas Chromatography, Advances in Chromatography Vol. IV, Ed. J. C. Giddings, Marcel Dekker, New York, p. 207, 1967.

18. Ettre, L. S. and Purcell, J. E., Porous-Layer Open Tubular Column-Theory, Practice, and Applications, Advances in Chromatography Vol. 10, Ed. J. C. Giddings, Marcel Dekker, New York, p. 1, 1974.

19. Tsuda, T. and Novotny, M., Band-Broadening Phenomena in Microcapillary Tubes Under the Conditions of Liquid Chromatography, Anal. Chem., 50, 632, 1978.

20. Tsuda, T. and Novotny, M., Packed Microcapillary Columns in High Performance Liquid Chromatography, Anal. Chem., 50, 271, 1978.

21. Giddings, J. C., Dynamics of Chromatography, Marcel Dekker, New York, 1965.

22. Ginochan, G., Preparation and Operation of Liquid Chromatographic Columns of Very High Efficiency, J. Chromatog., 185, 3, 1979.

23. Grushka, E., Snyder, L. R., and Knox, J. H., Advances in Band Spreading Theories, J. Chromatog. Sci., 13, 25, 1975.

24. DeClerk, K., Smuts, T. W., and Buys, T. S., Ultimate Resolution in Open Tubular Columns, J. High Res. Chromatog., 2, 172, 1979.

25. Giddings, J. C., Principles of Column Performance in Large Scale Gas Chromatography, J. Gas Chromatog., 1, 12, 1963.

26. Huyton, F. H., VanBeersum, W., and Rijnders, G. W. A., Improvements in the Efficiency of Large Diameter Gas-Liquid Chromatography Columns, Gas Chromatography 1960, Ed. R. P. W. Scott, Butterworths, Washington, p. 224, 1960.

27. Giddings, J. C., Lateral Diffusion and Local Nonequilibrium in Gas Chromatography, J. Chromatog., 5, 61, 1961.

28. Giddings, J. C., Physico-Chemical Basis of Chromatography, J. Chem. Ed., 44, 704, 1967.

29. Giddings, J. C., The Role of Lateral Diffusion as a Rate-Controlling Mechanism in Chromatography, J. Chromatog., 5, 46, 1961.

30. Giddings, J. C., Manwaring, W. A., and Myers, M. N., Turbulent-Gas Chromatography, Science, 154, 7, Oct. 1966.

31. Pretorius, V. and Smuts, T. W., Turbulent Flow Chromatography: A New Approach to Faster Analysis, Anal. Chem., 38, 274, 1966.

32. Tijssen, R., Effect of Column-Coiling on the Dispersion of Solutes in Gas Chromatography, Part I: Theory, Chromatographia, 3, 525, 1970.

33. Tijssen, R. and Wittebrood, R. T., Effect of Column-Coiling on the Dispersion of Solutes in Gas Chromatography, Part II: Generalized Theory, Chromatographia, 5, 286, 1972.

34. Wong, A. K., McCoy, B. C., and Carbonell, R. G., Theory of Capillary Chromatography: Effect of Coiling and Interphase Mass Transfer, J. Chromatog., 129, 1, 1978.

35. Dewaele, C. and Verzele, M., Some LC Experiments with Capillary Columns, J. High Res. Chromatog., 1, 174, 1978.

36. Desty, D. H. and Douglas, A. A., Study of New Column Forms in Gas Chromatography, J. Chromatog., 158, 73, 1978.

37. Zerenner, E. and Larson, P., Results Presented at ExpoChem 1979, Houston, October 22, 1979.

38. Sandra, P. and Verzele, M., Experiments with Capillary Columns Having Unconventional Cross-Sectional Geometry, J. High Res. Chromatog., 3, 253, 1980.

39. Hofmann, K. and Halasz, I., Mass Transfer in Ideal and Geometrically Deformed Open Tubes, Part I: Ideal and Coiled Tubes with Circular Cross-Section, J. Chromatog., 173, 211, 1979.

40. Halasz, I., Mass Transfer in Ideal and Geometrically Deformed Open Tubes, Part II: Potential Application of Ideal and Coiled Open Tubes in Liquid Chromatography, J. Chromatog., 173, 229, 1979.

41. Hofmann, K. and Halasz, I., Mass Transfer in Ideal and Geometrically Deformed Open Tubes, Part III: Deformed Metal and Plastic Tubes, J. Chromatog., 199, 3, 1980.

42. Reifsneider, S. and Stevenson, B., Micropak Preparative Columns for Liquid Chromatography, Varian Instrument Applications, 9(3), 8, 1975.

43. Said, A. S., Efficiency of Composite vs. Conically Shaped Chromatographic Columns, J. High Res. Chromatog., 2, 63, 1979.

44. Snyder, L. R. and Dolan, J. W., Coated-Open-Tubular Chromatography with Flow Segmentation, Part I: Theory, J. Chromatog., 185, 43, 1979.

45. Klesper, E., Chromatography with Supercritical Fluids, Angew. Chem. Int. Ed. Engl., 17, 738, 1978.

46. Small, H., Hydrodynamic Chromatography: A Technique for Size Analysis of Colloidal Particles, J. Coll. Interface Sci., 48, 147, 1974.

47. Novotny, M., Microcolumns in Liquid Chromatography, Paper presented at 10th Ohio Valley Chromatography Symposium, Hueston Woods, Ohio, June 22, 1978.

48. Brough, A. W. J., Hillman, D. E., and Perry, R. W., Capillary Hydrodynamic Chromatography--An Investigation into Operational Characteristics, J. Chromatog., 208, 175, 1981.

49. Ward-Smith, A. J., Internal Fluid Flow: The Fluid Dynamics of Flow in Pipes and Ducts, Clarendon Press, Oxford, 1980.

50. Yu, J. S., An Approximate Analysis of Laminar Dispersion in Circular Tubes, J. of App. Mech., 98, 537, 1976.

51. Friedman, M., Gillis, J., and Liron, N., Laminar Flow in a Pipe at Low and Moderate Reynolds Numbers, App. Sci. Res., 19(b), 426, 1978.

52. Jeffrey, G. B., The Two-Dimensional Steady Motion of a Viscous Fluid, Phil. Mag., Ser. b, 29, 455, 1915.

53. Hamel, G., Spiralförmige Bewegungen zäher Flüssigkeiten, Jahresbericht der Deutschen Mathematiker-Vereinigung, 25, 34, 1916.

54. Rosenhead, L., The Steady Two-Dimensional Radial Flow of Viscous Fluid Between Two Inclined Plane Walls, Proc. Roy. Soc., A, 175, 436, 1940.

55. Millsaps, K. and Pohlhausen, K., Thermal Distributions in Jeffrey-Hamel Flows Between Nonparallel Plane Walls, J. Aeronaut. Sci., 20, 187, 1953.

56. Abramowitz, M., On Backflow of a Viscous Fluid in a Diverging Channel, J. Math. Phys., 28, 1, 1949.

57. Pohlhausen, K. Zur Näherungsweisen Integration der Differential-gleichung der Grenzschict, Z. Angew. Math. Mech. 1, 252, 1921.

58. Goldstein, S., Modern Developments in Fluid Dynamics, Dover Publications, Inc., New York, Vol. 1, 106, 1965.

59. Milne-Thomson, L. M., Theoretical Hydrodynamics, Macmillan, New York, 1960.

60. Cohen, M. J. and Ritchie, N. J. B., Low-Speed Three-Dimensional Contraction Design, J. Roy. Aeronant. Soc., 66, 231, 1962.

61. Kachhara, N. L., Wilcox, P. L., and Livesey, J. L., A Theoretical and Experimental Investigation of Flow Through Short Axisymmetric Contractions, Fifth Anstralasian Conference on Hydraulics and Fluid Mechanics Conference Proceedings, Vol. 1, 82, Eds. D. Lindley and A. J. Sutherland, Univ. of Canterbury, Christchurch, New Zealand, 1974.

62. Lee, J. S. and Fung, Y. C., Flow in Nonuniform Small Blood Vessels, Microvascular Research, 3, 272, 197 .

63. Gibson, A. H., On the Flow of Water Through Pipes and Passages Having Converging or Diverging Boundaries, Proc. Roy. Soc., A, 83, 1910.

64. Patterson, G. N., Modern Diffuser Design, Aircraft Engineering, 10, 267, 1938.

65. Ackeret, J., Aspects of Internal Flow, Fluid Mechanics of Internal Flows, Ed. G. Sovran, Elsevier Publishing Co., New York, p. 1, 1967.

66. Ackeret, J., Grenzschichten in Geraden und Gekrümmten Diffosoren, IUTAM-Symposium Freibing/Br. Ed. H. Görtler, 22, 1957.

67. Sprenger, H., Messungen an Diffusoren, VDI-Berichte 3, 10, 1955.

68. Kline, S. J., Abbott, D. E., and Fox, R. W., Optimum Design of Straight-Walled Diffusers, J. Basic. Eng., Trans. ASME, 31, Series D, 1959.

69. Schlichting, H. and Gersten, K., Berechnung der Strömung in Rotationsymmetrischen Diffusoren mit Hilfe der Grenzschicht-theorie, ZFW, 9, 135, 1961.

70. Clayton, B. R. and Massey, B. S., Flow Visualization in Water--A Review of Techniques, J. Sci. Instrum., 44, 2, 1967.

71. Merzkirch, W., Flow Visualization, Academic Press, London, 1974.

72. Asanuma, T., Editor, Flow Visualization, International Symposium on Flow Visualization, Tokyo, 1977, Hemisphere Publishing Corporation, Washington, D.C., 1979.

73. Dirkes, W. E., The Effects of 1,1-Difluoroethane on the Adorptivity of Glass Capillary Tubing, University of Dayton Research Institute, UDR-DR-79-07, May 1979.

74. Dirkes, W. E., A Study of Surface Roughening and Deactivation Techniques for Glass Open Tubular Gas Chromatographic Columns, University of Dayton Research Institute, UDR-TR-79-02, January 1979.

75. Dirkes, W. E., Rubey, W. A., and Pantano, C. G., The Formation of a Silica-Rich Surface Using Sulfur Dioxide in Drawn Glass Capillaries, J. High Res. Chromatog., 3, 303, 1980.

☆ U.S.Government Printing Office: 1984 — 759-062/619

END

FILMED

2-84

DTIC